Scientific Research Publishing

Retraction Notice

Title of retracted article:	**Hydraulic Performance and Effectiveness of Trees, Shrubs and Grasses as Riparian Vegetations in Reducing Flow Velocity near Riverbanks, Subsequent to Riparian Erosion and Sediment Generation Control in HumidTropics**
Author(s):	Moïse Ndekezi, Ayalew Talema Legass, Jan Diels
* Corresponding author.	Email: mosnde06@yahoo.com
Journal:	Journal of Environmental Protection
Year:	2016
Volume:	7
Number:	9
Pages (from - to):	1157 - 1182
DOI (to PDF):	http://dx.doi.org/10.4236/jep.2016.79104
Paper ID at SCIRP:	69672
Article page:	http://www.scirp.org/Journal/PaperInformation.aspx?PaperID=69672
Retraction date:	2016/-09-27

Retraction initiative (multiple responses allowed; mark with **X**):

X All authors
☐ Some of the authors:
☐ Editor with hints from
- O Journal owner (publisher)
- O Institution:
- O Reader:
- O Other:

Date initiative is launched: 2016-09-21

Retraction type (multiple responses allowed):

☐ Unreliable findings
- O Lab error
- O Inconsistent data
- O Analytical error
- O Biased interpretation
- O Other:

☐ Irreproducible results
☐ Failure to disclose a major competing interest likely to influence interpretations or recommendations
☐ Unethical research

☐ Fraud
- O Data fabrication
- O Fake publication
- O Other:

☐ Plagiarism ☐ Self plagiarism ☐ Overlap ☐ Redundant publication *
☐ Copyright infringement ☐ Other legal concern:

☐ Editorial reasons
- O Handling error
- O Unreliable review(s)
- O Decision error
- O Other:

X Other:

Results of publication (only one response allowed):

☐ are still valid.
X were found to be overall invalid.

Author's conduct (only one response allowed):

☐ honest error
☐ academic misconduct
X none (not applicable in this case – e.g. in case of editorial reasons)

* Also called duplicate or repetitive publication. Definition: "Publishing or attempting to publish substantially the same work more than once."

History
Expression of Concern:
☐ yes, date: yyyy-mm-dd
X no

Correction:
☐ yes, date: yyyy-mm-dd
X no

Comment:

The paper is withdrawn by the authors for the personal reason.

This article has been retracted to straighten the academic record. In making this decision the Editorial Board follows COPE's Retraction Guidelines. Aim is to promote the circulation of scientific research by offering an ideal research publication platform with due consideration of internationally accepted standards on publication ethics. The Editorial Board would like to extend its sincere apologies for any inconvenience this retraction may have caused.

Editor guiding this retraction: Prof. Thangarasu Pandiyan
(function e.g. EiC, Journal of Environmental Protection)

Journal of Environmental Protection, 2016, 7, 1157-1182
Published Online August 2016 in SciRes. http://www.scirp.org/journal/jep
http://dx.doi.org/10.4236/jep.2016.79104

Scientific Research Publishing

Hydraulic Performance and Effectiveness of Trees, Shrubs and Grasses as Riparian Vegetations in Reducing Flow Velocity near Riverbanks, Subsequent to Riparian Erosion and Sediment Generation Control in Humid Tropics

RETRACTED

Moïse Ndekezi[1], Ayalew Talema Legass[2], Jan Diels[3]

[1]Department of Civil, Environmental and Geomatic Engineering, College of Science and Technology, University of Rwanda, Kigali, Rwanda
[2]Department of Horticulture and plant science, College of Agriculture and Veterinary Medicine, Jimma University, Jimma, Ethiopia
[3]Department of Earth and Environmental Sciences, Division of soil and water management, Katolieke Universiteit Leuven (KULeuven), Leuven, Belgium
Email: mosnde06@yahoo.com, mndekezi@ur.ac.rw

Received 27 June 2016; accepted 7 August 2016; published 11 August 2016

Abstract

This paper described a methodology followed to quantify hydraulic performance and effectiveness of trees, shrubs and grasses in reducing flow velocity near riverbanks with the help of a field experiment conducted in Jimma zone (South-West Ethiopia) which fell in the humid tropics. Jimma zone is one of the regions with most eroded riverbanks, increasing population pressure, torrential rainfall, rugged topography and lack of proper land management. These problems impose two major impacts as *in-situ* soil loss and siltation of hydroelectric dams, consequent to reduction in efficiency of hydropower generation. In Ethiopia, several tons of sediments are transported annually from the highlands to downstream rivers and entail huge costs to Ethiopia such as dredging costs of clogged channels, desludging of reservoirs and hydroelectric dams. One of the primary sources of sediments for the dams is associated with riverbank erosion. The most sustainable and economical means of stabilizing riverbanks is the use of appropriate vegetation. This study was carried out on locally available, eco-friendly and economically motivating vegetation species that could be planted by all local people on banks of rivers that run along their lands. Six vegetation species were selected and contrasted with bare bank treatment: *Salix purpurea* and *Sesbania ses-*

How to cite this paper: Ndekezi, M., Legass, A.T. and Diels, J. (2016) Hydraulic Performance and Effectiveness of Trees, Shrubs and Grasses as Riparian Vegetations in Reducing Flow Velocity near Riverbanks, Subsequent to Riparian Erosion and Sediment Generation Control in Humid Tropics. *Journal of Environmental Protection*, **7**, 1157-1182.
http://dx.doi.org/10.4236/jep.2016.79104

ban **as shrubs;** ***Pennisetum purpureum*** **and** ***Pennisetum macrourum*** **as grasses and finally** ***Syzigium guineense*** **and** ***Saccharum officinarum*** **as trees. This assessment was achieved with the help of a field artificial trapezoidal flume with water from a diverted river and data were collected with the help of a 10-MHz Acoustic Doppler Velocimeter and Horizon ADV software and were analyzed with Win ADV and Microsoft Excel. The results revealed that the vegetation characteristics and planting arrangements affected much their impact on water flow velocity. Almost all vegetations showed power in reducing lateral shear stresses responsible for riverbank erosion except** ***Saccharum officinarum*** **and** ***Syzygium guineense*** **which were less effective due to their big diameters compared to the other species. They also showed that** ***Salix purpurea*****,** ***Pennisetum macrourum*** **and** ***Sesbania sesban*** **were the most effective species to reduce water velocities near the banks due to their small diameters, stem density and leaves' density. However, less leafy species didn't increase surface roughness, the major parameter, to reduce water flow. As the fluvial erosion control is an intensive project, it is recommended that the participatory involvement of local people should be encouraged to cover maximum possible area.**

Keywords

River Flow Velocity, Riverbank Erosion, Riparian Vegetations, Vegetation Characteristics, Humid Tropics

RETRACTED

1. Introduction

Excess sedimentation of man-made water bodies (fish ponds, reservoirs and dams) through rivers running in different catchments is a significant problem worldwide. Multiple geomorphic processes generate sediment, with water acting as the primary erosion, transport, and deposition agent (**Figure 1**). The Gilgel Gibe catchment is one of those affected catchments and one of the land resources of great economic importance for Ethiopia. It provides water for a cascade of the Gibe hydroelectric power plants (**Figure 2**), namely GIBE I (operating), GIBE II (operating), GIBE III (operating), GIBE IV (under study) and GIBE V (under study) that help the country in self-satisfying in hydroelectric power in the country, Ethiopia [1]. The 4225 km² catchment is occupied and cultivated by a large number of smallholding farmers. Poor land management practices coupled with the rugged topography and erosive rainfall regime in the area pose major threats both to the livelihood of the farmers and the life span of the dam because of siltation. River bank degradation (**Figure 3**) is one major point of sediment generation and transport, which is subsequent to the decrease of their storage capacity and which, in turn, presents impact on hydropower generation. In Ethiopia, the phenomenon is highly aggravated due to increasing population pressure, torrential rainfall, rugged topography and lack of proper land management. The erosion problem imposes two fold impacts via soil loss *in-situ* and *ex-situ* siltation of hydroelectric dams. The problem of silts and sediments is the major drastic threatening factor of their life span and storage capacity [2].

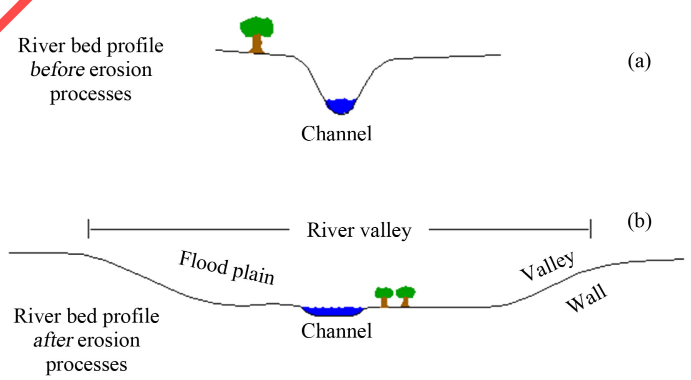

Figure 1. River morphological shape change due to erosion from steep bank slopes (a) to gentle slopes (b), adapted from [18].

In order to protect these hydropower dams from siltation and sedimentation, different mechanisms should be taken under consideration like preventing sediments from highlands and erodibility of river banks and different land restoration methods. Erodibility of river banks (**Figure 3**) and their daily exposure to water flow waves make the drastic yield of sediments in rivers [3]. Many findings revealed that riparian vegetations had much power on regulating water flow velocities in channels and rivers. They play an important role in modifying flow characteristics (such as velocity distribution, Reynolds number, manning coefficient and so on) compared with non vegetated conditions in rivers [4].

The riparian species stabilize the riverbanks through three main mechanisms: hydrological (interaction with river overflow by their stems, branches and leaves; by interception; water uptake of water from deep soil layers; water storage in large roots, in stem, in branches and leaves; filtration and evapotranspiration), hydraulic (by increasing surface roughness of riverbanks) and mechanical (soil strength induced by the root system) [5] and [6]. Laften [7]

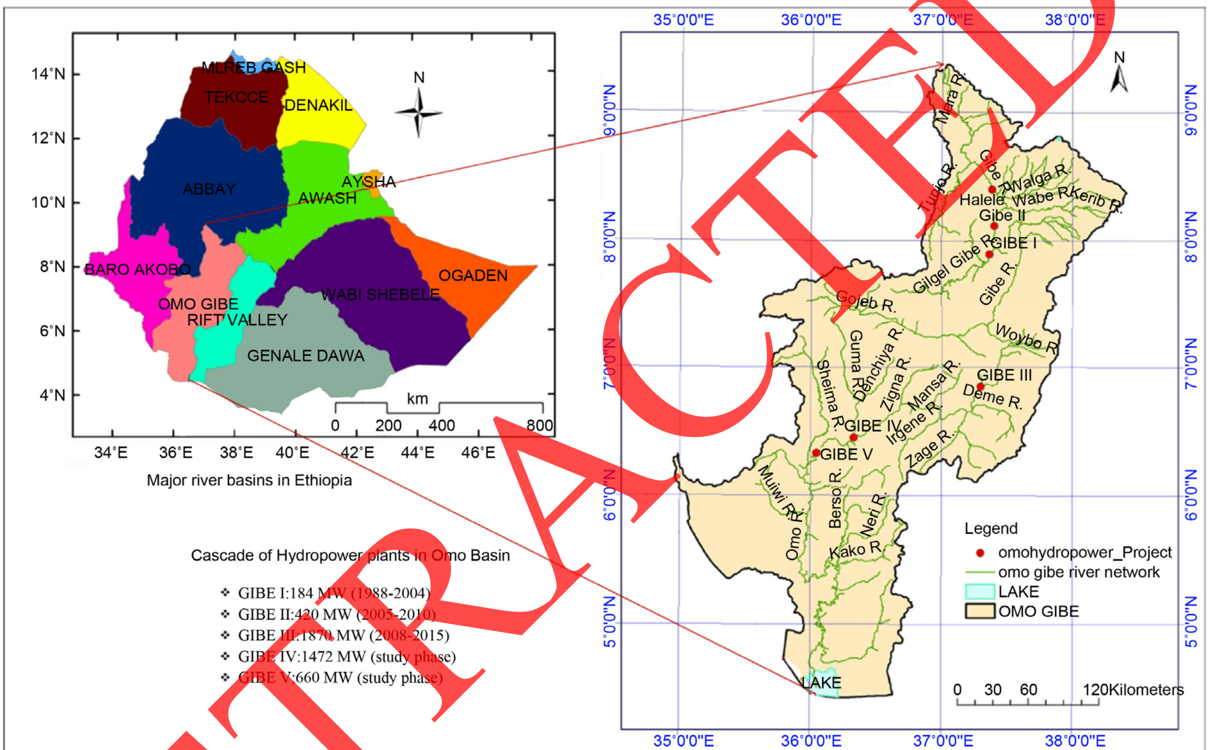

Figure 2. The Omo Gibe River Basin showing the main and tributaries of river network system of the watershed, and hydropower generation projects (source: [1]).

Figure 3. River bank erosion, in Gilgel Gibe catchment, causing sediments loading (d), and bank collapses (c) and performance of a vegetated bank portion (a) in diverting water flow (d), adapted from [21].

and Vought [8] identified that forestation and grass planting could increase surface-roughness and reduce: the impact of raindrops' ability of running water to detach and transport sediments. Plantation of riparian vegetations is viewed as the most effective mitigation measure in fighting against riparian erosion [5] [9]-[11].

They do not affect only flow hydraulics but also hydrological impacts physically like interaction with overflow by stems, branches and leaves generating turbulence; increase in turbulence as a consequence of root exposure; increase of substrate macro-porosity by roots which prevents slaking; stem flowing due to excess rainfall; etc. and physiologically like water storage in large roots, in stem, in branches and leaves; evapotranspiration and hydraulic lift, uptake of water from deep soil layers [12]-[14].

Rivers run long distances, in different people's lands with different management. One can grow riparian vegetations on banks of his concerns and others do not. River bank erosion has been well-known for long time to exercise naturally a significant influence on the bank morphology and to fight against its needs to conjugate efforts. "*People cannot stop erosion*; *they can only speed it up or slow it down. It is the nature of rivers and streams to move and there is no guarantee for complete success of any erosion control project but its alleviation to a non-detrimental status is possible*" [15]. River bank erosion is the unique process in channel systems, which is closely linked to other processes such as sediment transport and deposition, water flow dynamics and lateral runoffs [16]. It changes a river into four dimensions: lateral, longitudinal, vertical and temporal. The most visible dimensional change is lateral, which is caused by bank erosion [17]. It is one of most critical type of environmental problems because it causes much sediments loading and depends on amount of rainfall, soil structure, river morphology, topography and flooding as shown in **Figure 1** adapted from [18] and **Figure 3** adapted from [19].

In a nutshell, extensive researches have been done to determine the mechanism of interaction between riparian vegetation and water flow velocity in open channels. Several methods have been accepted and many findings revealed that riparian vegetations have much power on regulating water flow velocities in channels and rivers [5] [10] [12] and [20]. The challenge from all the previous findings was to discern vegetation parameters that presented influence on water flow velocities, their quantifiable magnitudes, assessment techniques, assumptions and flow conditions under which vegetations were subjected to. This present study was undertaken to try finding answers to these questions by relating vegetation characteristics (type, stem diameter, stem density, leafiness, flexibility and planting arrangement) to water flow velocity parameters (manning's surface roughness, hydraulic radius, channel bed slope, turbulence intensities and Reynolds shear stresses).

2. Study Area

2.1. Description of Location

The field experiment (**Appendix 1**) was conducted in an artificial flume dug near on Meti river, the tributary to Gilgel Gibe river in Gilgel Gibe catchment (**Figure 4**), in Seka Chekorsa district, Southwest Ethiopia, about 380 km from Addis Ababa. The catchment covers an area of about 5500 km^2 with an altitude that varies between 1096 and 3259 m above mean sea level. It is approximately located between 7˚22'72" and 7˚34'84" latitude N and between 37˚21'05" and 37˚28'80" longitude E [21]. The bulk of the catchment is located in the south of Jimma zone, one of zones of Oromia region. The main city in the catchment is Jimma, located at an altitude of 1800 m above the mean sea level. The Gilgel Gibe is the main river of the catchment and is cut by a cascade of Gilgel Gibe hydroelectric dams [1]. These dams need to be protected from being filled up by silts and sediments resulting from river bank erosion (**Figure 1**) and (**Figure 3**).

2.2. Description of Climate

The climate of Jimma zone, where the catchment is located, is tropical humid (**Appendix 8**) with average annual temperature of 19.2˚C. The annual rainfall of the Gilgel Gibe catchment varies from a minimum of 1300 mm near the confluence with the Great Gibe River, to a maximum of about 1800 mm in the Utubo and Fego mountains with annual average of is 1624 mm. The 60% of the total amount of annual rainfall occurs between June and September, 30% from February to May, and only 10% between October to January [22]. The rainfall pattern in the Catchment is distributed over only one season with an average of 20.5˚C in April, the warmest month and 17.7˚C in December, the coldest month. **Figure 5** and **Figure 6** represent and summarize the average annual distribution of precipitation and mean temperature at meteorological station of Jimma Airport, calculated with daily data from 1981 to 2005.

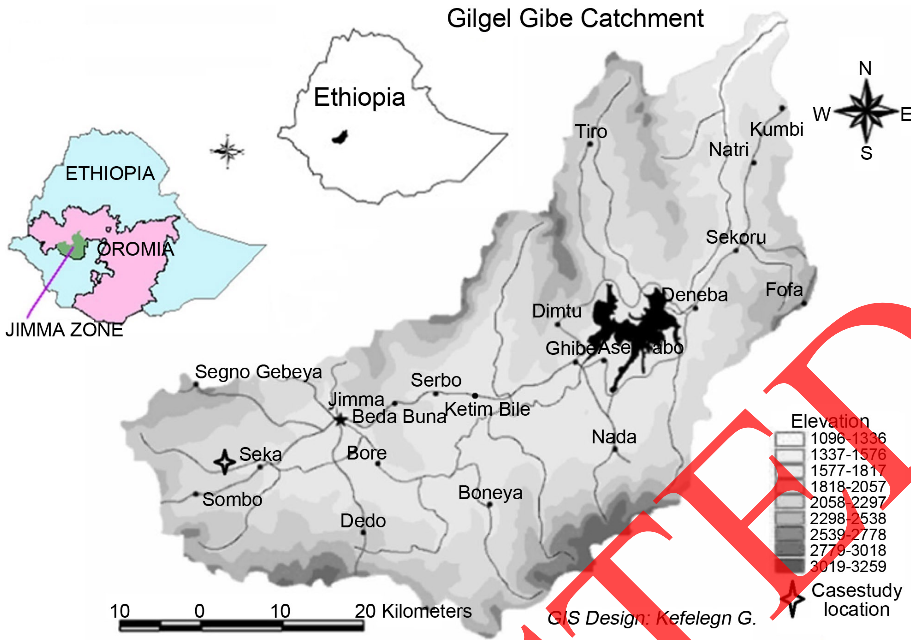

Figure 4. Gilgel Gibe catchment, the sub-catchment of Omo Gibe basin illustrated in Ethiopian hydrographic basins. Adated from [21].

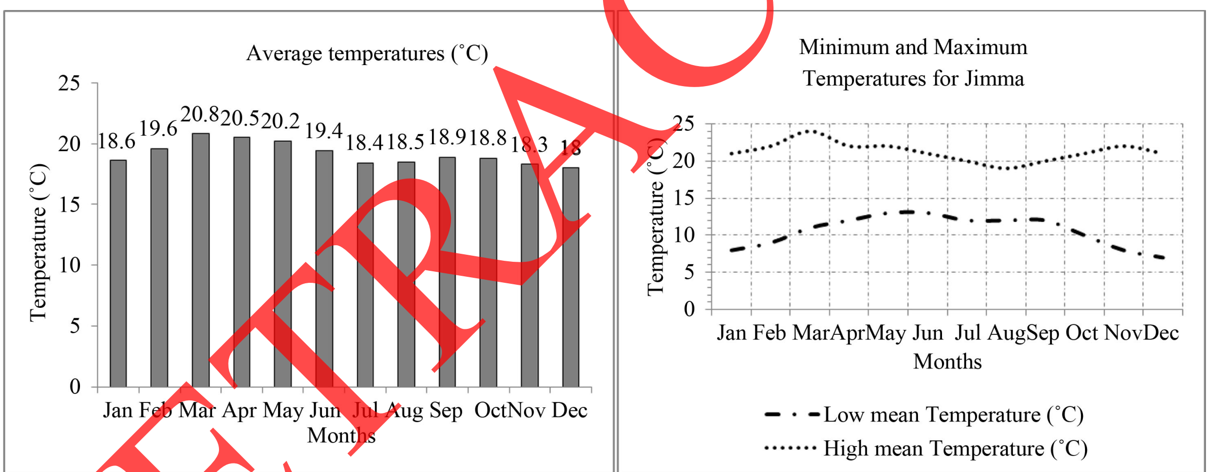

Figure 5. Annual temperature variation in Jimma.

3. Materials and Methods

3.1. Experimental Layout

The experiments were conducted in a 25 m long trapezoidal field flume, 1.20 m deep, 0.8 m bottom-wide, 2.9 m top-wide, with a bed slope of 0.0003 m/m and a side slope length of 1.45 m long with side slope equal to 0.952 m/m (**Figure 7** and **Figure 8**). Water flowing in the channel, was taken from a weir dam built to divert water flow of a natural stream "Meti" in the Gilgel Gibe catchment (**Figure 7** and **Figure 9**).

To minimize the turbulence and get uniform flow, a bundle of 50 cm long PVC tubes with a diameter of 50 mm was inserted at downstream of upper sluice gate. The first and the last 5 m and 8.5 m long sections of the channel were used as a transition zone to stabilize the flow (the length of the transition zone is rearranged after the first design is made). The 6 m long mid-section had similar base with the flow straightener except the presence of plant fixing metallic boxes covered with a soil layer (**Figure 10**).

After having finished a channel preparation, insertion of vegetations started. All measurements were taken for

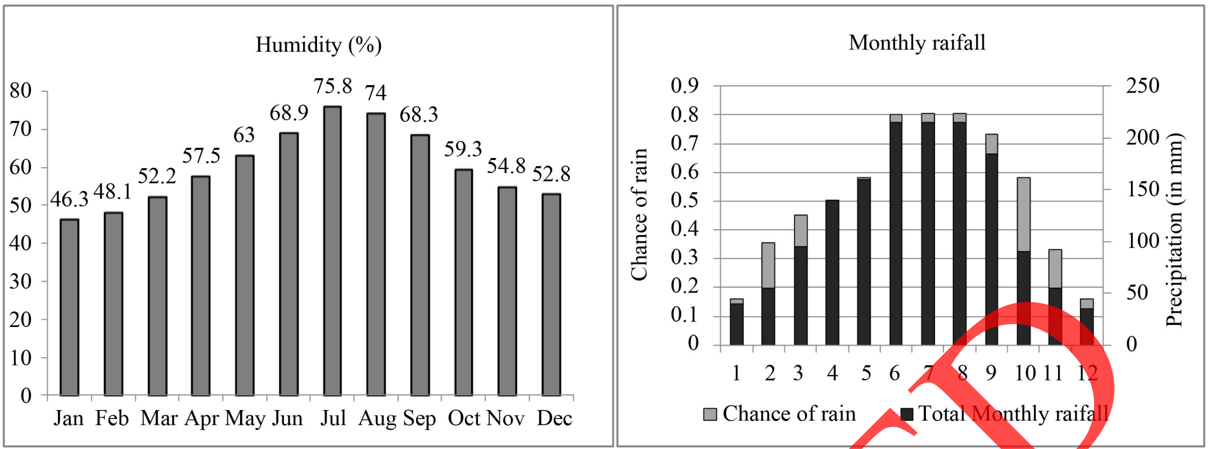

Figure 6. Annual humidity and rainfall variation in Jimma.

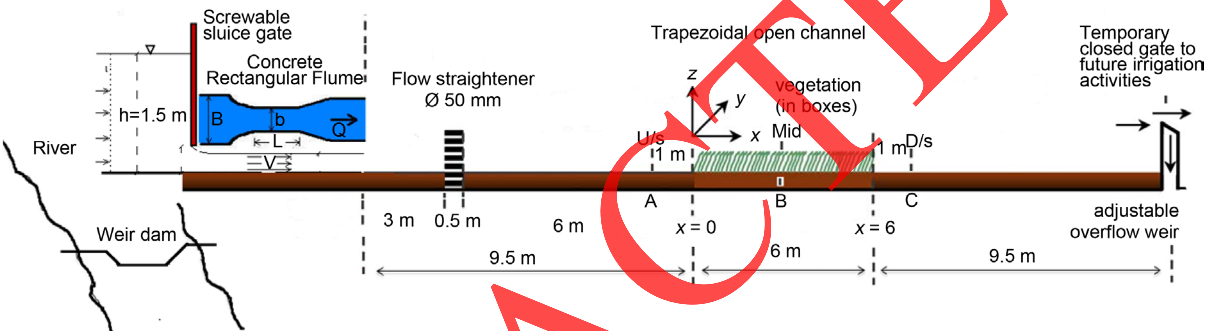

Figure 7. Longitudinal view of experimental set-up (not to scale) (source: adapted from Citation number 14 (Järvela, 2005)).

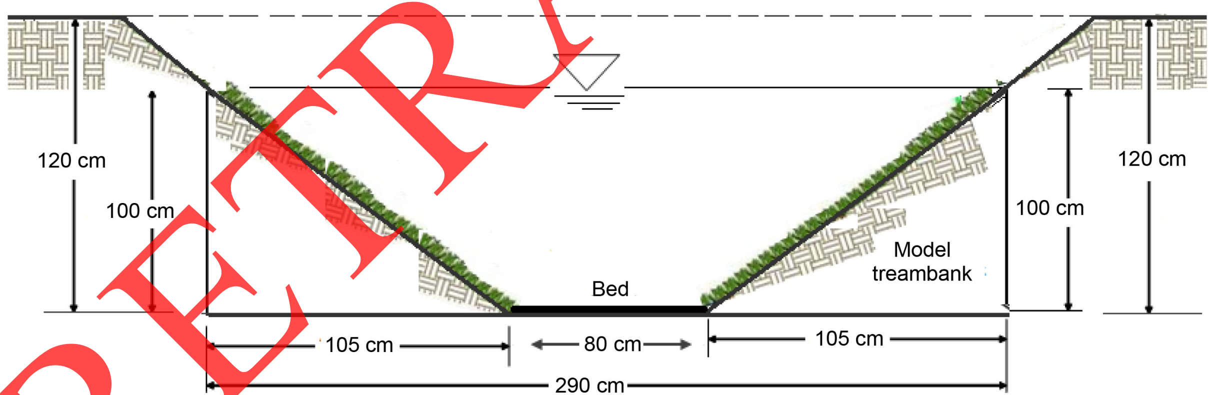

Figure 8. Cross-sectional view of the vegetated channel section.

each species one after another. The explored vegetations (Figure 11) were pre-planted prior to this study in the research area at downstream of the testing flume. Their densities (no. of stems/m^2) and their external diameters measured with the vernier caliper were taken into consideration. Their distribution as shown on Figure 12 was follows: *Pennisetum purpureum* (commonly known as elephant grass) covered the test area with an average stem density of 49 stems/m^2, 256 stems/m^2 for *Pennisetum macrourum* (commonly known as African feather grass and locally known as Jejeba), 25 stems/m^2 for *Saccharum officinarum* (commonly known as sugar cane and locally known as shenkora), 49 stems/m^2 for *Salix purpurea* (commonly known as Purple willow and locally known as Akeya (Aleltu, in Oromo), 42 stems/m^2 for *Sesbania sesban* commonly known as Egyptian pea) and finally 35 stems/m^2 for *Syzygium guineense* commonly known as Snak bean tree and locally known as Dokma in Amharic, Bedesa in Oromo).

Figure 9. The weir dam across Meti river (a), upstream sluice gate structure (b), artificial flume (c) and the downstream overflow control gates (d).

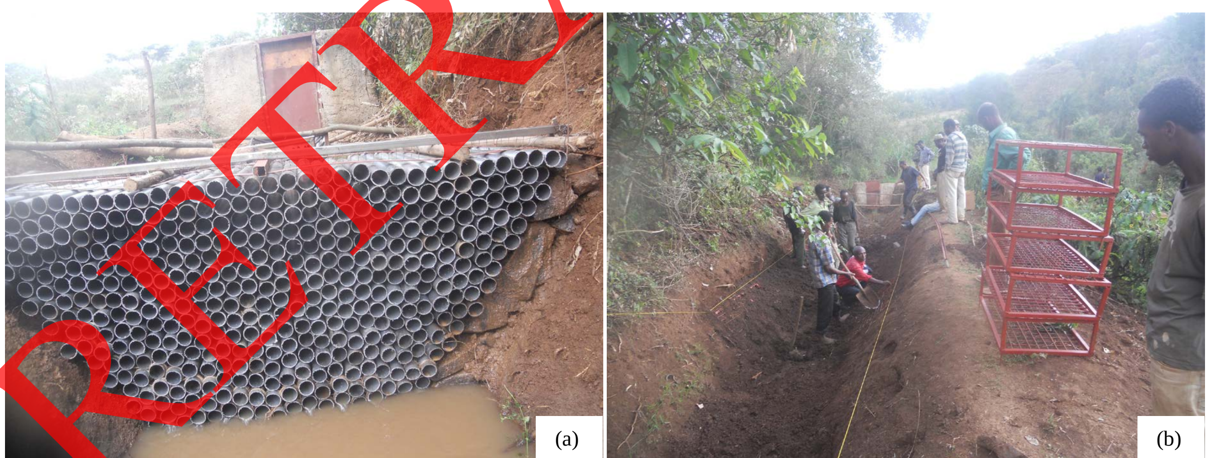

Figure 10. Flow straightener composed of bundles of pieces of Ø 50 mm PVC pipes (a) and plant fixing metallic boxes buried on the side walls of the channel (b).

3.2. Measurements Procedures and Techniques

After insertion of vegetations, measurements of velocity data points started. During the whole experimental work, nine treatments were carried out (**Figure 13**). For each treatment, there are three data collection cross sections: one at 1 m away at upstream of a vegetated channel, second in the middle of vegetated section and third at 1 m away from vegetated area in the downstream direction. In each section, eleven profiles were collected: 3 profiles (P1, P2 and P3) perpendicular to the bed with 8 data points each and 8 slanted profiles named as (SL-1,

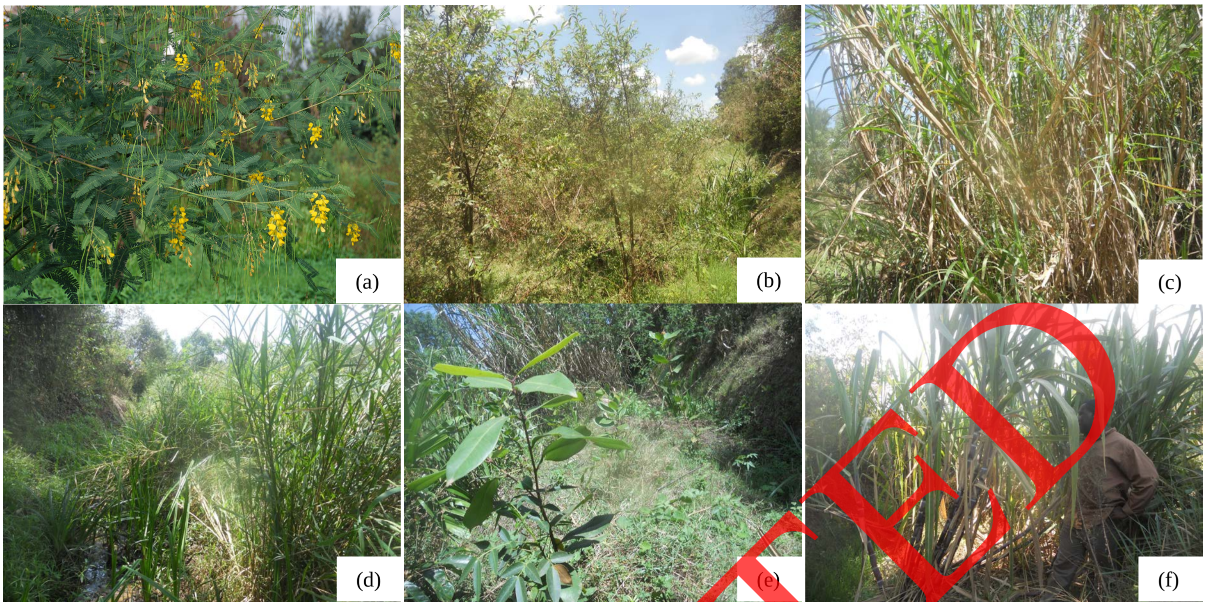

Figure 11. Tested vegetation species: (a) *Sesbania sesban*, (b) *Salix purpureum*, (c) *Pennisetum purpureum*, (d) *Pennisetum macrourum*, (e) *Syzygium guineense*: young species, (f) *Saccharum officinarum*.

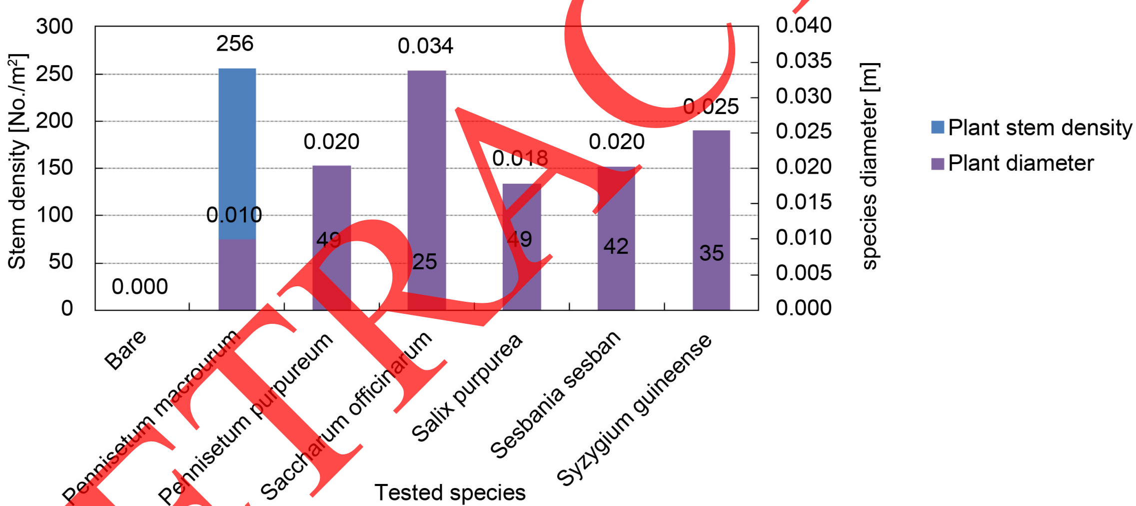

Figure 12. Stem densities and diameters of the studied vegetations.

SL0, SL1, SL2, SL3, SL4, SL5 and SL6) perpendicular to the bank of the channel with 8 data points for SL-1 decreasing to one for SL6 respectively (**Figure 14**). The first and last three velocity data points were taken perpendicular to the channel bed starting at 15 cm from the bed and below water level. In-between data points were measured at 10 cm of vertical difference respectively. The same procedure was followed for the slanted profiles. The reason of leaving 15 cm above river bed and river bank was due to technical functionality of ADV instrument used. When the 3D probe is immersed in water, the rays of four electro-acoustic transducers meet in one point called "the measurement volume": one in central acts as transmitter and 3 remaining as receivers (**Figure 15 (h)**). The central transmitter sends one very short acoustic pulse on soil particles moving in the fluid, and record its return signal (*i.e.* the reflection off particles in the fluid contained in sampling volume), and then transmit a second pulse, identical to the first, at a short time later. Each return is detected by acoustic receivers focused in a remote sampling volume (**Figure 15 (j)**). The distance from the transmitter to the sampling volume in the 10 MHz Sontek ADV is about 10 cm. Therefore, first measurements can't be taken at 10 cm because sampling volume can be coincided with river bank or river bed.

Figure 13. Different vegetations treatments tested on banks of the testing flume: (a) *Pennisetum purpureum*, (b) *Syzygium guineense*: young species, (c) *Saccharum officinarum*: young species (d) *Salix purpurea*, (e) *Pennisetum macrourum*, (f) *Sesbania sesban*, (g) Barebank treatment, (h) *Syzygium guineense*: grown up species and finally (i) *Saccharum officinarum*: grown up species.

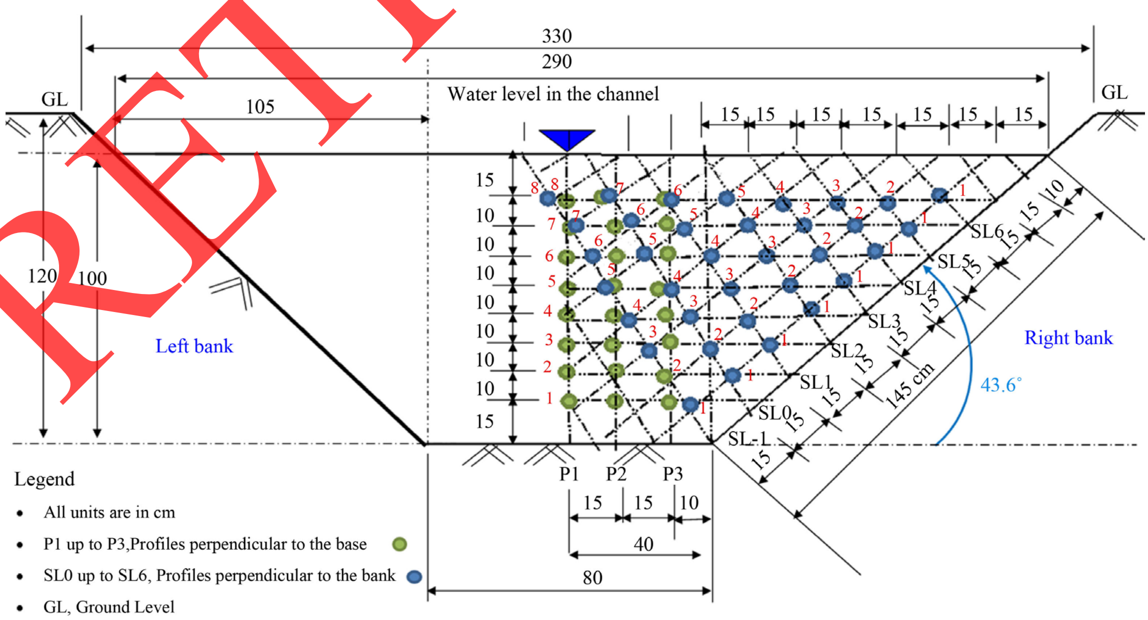

Figure 14. Sketch showing all profile data points in the channel (not to scale).

3.3. Data Collection Tools

A 10-MHz Acoustic Doppler Velocimeter (**Figure 15**) mounted on suitable structured wood and steel frame across the measuring section of the channel and Horizon ADV software were used to collect the 3D mean instantaneous velocities and fluctuations (**Figure 16**) at a single point located at 10 cm from the probe, connected to the computer via a processing card. This data acquisition program (Horizon ADV) is windows-based software for that offers a flexible and dynamic user interface designed to easily guide the user through the data collection and display process [23]. It configures ADV systems, registers data collected and displays data files collected using ADV system. ADV system records three basic data types with each sample: velocity, signal strengths and correlation coefficient scores (**Appendix 2**). Each of these data has 3 values to make up a total of nine values recorded simultaneously: three velocity components, their corresponding signal strength values and three correlation coefficient scores. Velocity data were almost exclusively the parameter of most interest.

However, the other two parameters hold valuable data quality information. Signal strengths and correlations were used primarily to determine the quality and accuracy of the velocity data. During data collection, Horizon ADV helped in data visualization and judgment of their quality and this stage is called "data pre-processing

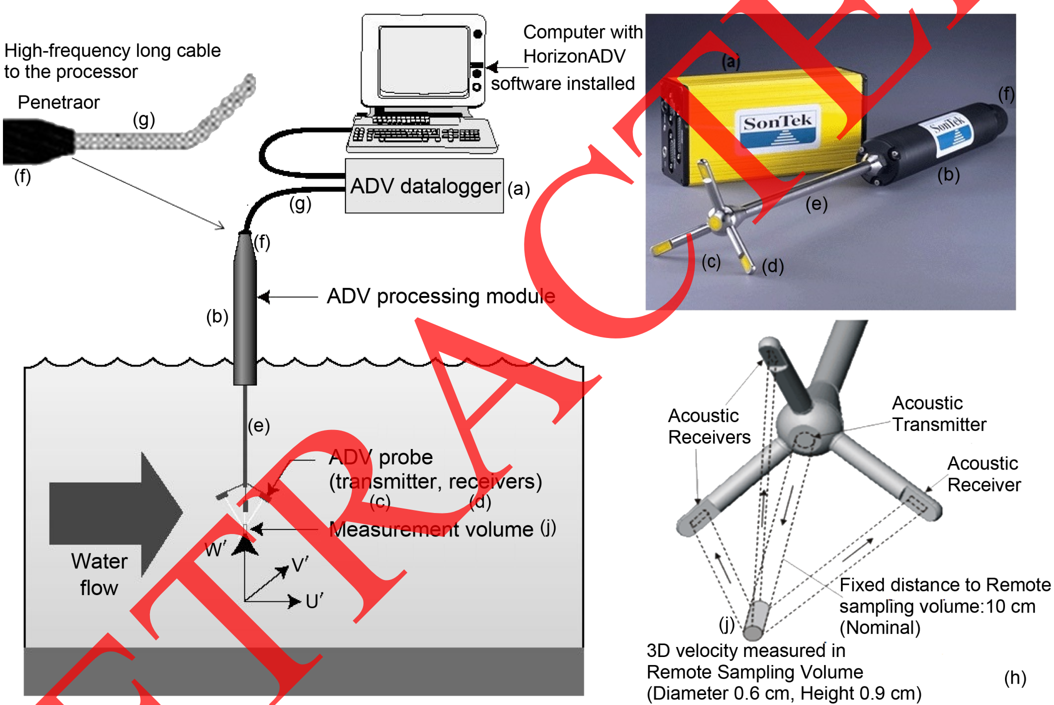

Figure 15. Schematic diagram of general setup of ADV and computer in water flow for direct flow measurements of the variable velocity components in the x, y and z directions.

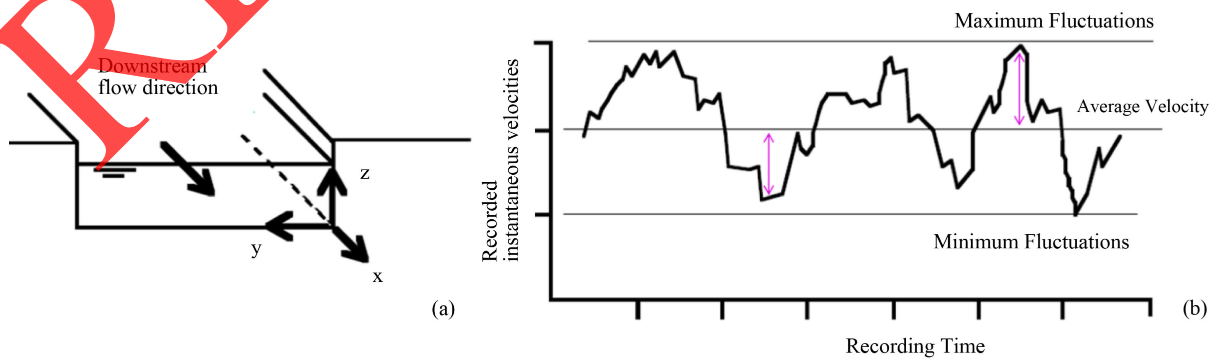

Figure 16. The referential coordinate system for the turbulent flow equations Velocity record of unsteady motion of turbulent flow (source: adapted from [27]).

technique". With Horizon ADV, data quality was accessed at the same time of data sampling by checking data quality indicators: Signal-to-noise ratio amplitudes (SNRs) in dB (decibel) units with values greater or equal to15 dB as good values and correlation coefficient scores (0% to 100%) with values greater or equal to 70% as good values [24]. As it can be viewed in **Appendix 2**, correlation coefficient score is a direct measurement of ADV data quality. It is a measure of how well the particles inside the sampling volume maintain their relative position with respect to each other such that the strength and relative phases of the individual pulse echoes are unchanged from one pulse to the next [25]. It is reported as a percentage, with 100% meaning that perfect phase coherence is maintained between the pulses and noise is inexistent. When the signal is dominated by noise and no phase coherence exists, the correlations coefficient is 0%, an indicator of poor data quality. The checking of data quality was done throughout data collection. With this, it was easy to discard adv files of less quality.

The ADV systems give data stored in file with extension .adv and these advfile.adv data files from the instrument are automatically converted to the SDS format (with extension.sds). The Horizon ADV does never modify or delete originaladvfile.adv data files. The file.sds contains all data points of each advfile.adv file and can be visualized in data grid on computer program screen.

For each measurement, data points were acquired at a sampling-reporting rate of 25 Hz and data were good if sapling rate was as high as 25 Hz and the acoustic frequency was 10 MHz [26]. The 3-D velocity range was set to ±250 cm/s. The velocity components *u*, *v* and *w* corresponding to the stream-wise (X), span-wise (lateral) (Y) and vertical (X) directions were recorded respectively (**Figure 15** and **Figure 16**) and a 60-second sampling period was set for each test run. The general data collection setup of sampling equipment complex was composed of a 10-MHz ADV Field Splashproof processor 1), signal conditioning module 2) and Velocimeter probe 3) with one acoustic transmitter and signal receivers 4), stem 5), penetrator 6), a 20 m long high-frequency cable connecting conditioning 7) (**Figure 15**).

3.4. Data Analysis Tools

The collected data were analyzed with Win ADV as post-processing software and Microsoft Excel as manipulation tool for the post-processed data from Win ADV. Win ADV software is a windows-based viewing and post-processing utility for ADV files collected using Acoustic Doppler Velocimeter (ADV). It offers powerful filtering and processing options [28] and these options were used to deliver data in many variable formats for analysis. It helps to review data files, to identify anomalies caused by low signal strength or over-arranging of the ADV probe and to minimize the need for manipulating large quantities of time series data.

The outputs of Win ADV are average values for all variables and parameters. The raw data were filtered out using the following options:

- Data with average and minimum correlations between velocities was set to be greater than 70%,
- Average and minimum SNR was set greater than 15 dB,
- The option "Phase-space threshold despiking filter without replacing as described by [29] was checked and the option "Filter out communication errors" was checked.

The filtered data were stored as "filename ADV.Vf" and unfiltered data were stored as "filename ADV.VU". For each file, the summary statistics such as average *u*, *v*, and *w*, correlations, root mean square errors, signal to noise ratio, etc were calculated. Statistical summary information for each ADV file was stored in files named "Filtered.Sum" and "UnFilter.Sum", or the user may choose other filenames before processing the file like "Filtered_filename.sum" and "UnFilter_filename.sum". These files can be easily opened in Excel as "Filtered-filename.sum.xls".

Win ADV calculates many quantities but in this study, we were limited to the following velocity parameters.

3.4.1. Average Velocities

The average velocities were calculated as shown below:

$$\bar{u} = \frac{1}{n}\sum_{i=1}^{n} u_i;\ \ \bar{v} = \frac{1}{n}\sum_{i=1}^{n} v_i;\ \ \bar{w} = \frac{1}{n}\sum_{i=1}^{n} w_i \quad (1)$$

$$u' = u - \bar{u};\ \ v' = v - \bar{v};\ \ w' = w - \bar{w} \quad (2)$$

$$V_R \text{ or } V_{Total} = \sqrt{\left(\bar{u}^2 + \bar{v}^2 + \bar{w}^2\right)} \quad (3)$$

where:

$\bar{u}$, $\bar{v}$ and $\bar{w}$ are average velocity components (Time-averaged velocities) in XYZ coordinates; in m/s;
u_i, v_i and w_i are instantaneous flow velocities in XYZ coordinate system, in m/s;
u', v', w' are velocity fluctuations in XYZ coordinate system, in m/s;
V_R or V_{Total} is the total velocity or the Resultant of the three average velocity components, in m/s;
n is the total number of measurements.

3.4.2. Variances

The variances of all measurements in (m^2/s^2) as indicators of how data points are spread across a data set, were determined.

$$\sigma_u^2 = \frac{1}{n}\sum_1^n\left(u-\bar{u}\right)^2 = \frac{1}{n}\sum_{i=1}^n u'^2 = \overline{u'^2}\ \left(\text{m}^2/\text{s}^2\right) \tag{4}$$

$$\sigma_v^2 = \frac{1}{n}\sum_1^n\left(v-\bar{v}\right)^2 = \frac{1}{n}\sum_{i=1}^n v'^2 = \overline{v'^2}\ \left(\text{m}^2/\text{s}^2\right) \tag{5}$$

$$\sigma_w^2 = \frac{1}{n}\sum_1^n\left(w-\bar{w}\right)^2 = \frac{1}{n}\sum_{i=1}^n w'^2 = \overline{w'^2}\ \left(\text{m}^2/\text{s}^2\right) \tag{6}$$

where:

σ_u^2: The variance of the velocity fluctuations in streamwise direction in m^2/s^2;
σ_v^2: The variance of the velocity fluctuations in lateral direction in m^2/s^2 and;
σ_w^2: The variance of the velocity fluctuations in vertical direction in m^2/s^2.

3.4.3. RMS Turbulence Parameters

The root-mean-square of the turbulent velocity fluctuations (Figure 16) about the mean velocity were computed for use in determining turbulence intensities and levels of turbulent kinetic energy. The RMS values are equal to the standard deviation of the individual velocity measurements in x, y and z directions respectively. *RMSs* were considered as a measure of the violence of turbulent fluctuations to show how the velocities varied from the mean. They were determined in the following equations [20]:

$$RMS\left[u'\right] = \sigma_u = \sqrt{\frac{1}{n}\sum_{i=1}^n\left(u-\bar{u}\right)^2} = \sqrt{\frac{1}{n}\sum_{i=1}^n u'^2} = \sqrt{\overline{u'^2}}\ (\text{m/s}) \tag{7}$$

$$RMS\left[v'\right] = \sigma_v = \sqrt{\frac{1}{n}\sum_{i=1}^n\left(v-\bar{v}\right)^2} = \sqrt{\frac{1}{n}\sum_{i=1}^n v'^2} = \sqrt{\overline{v'^2}}\ (\text{m/s}) \tag{8}$$

$$RMS\left[w'\right] = \sigma_w = \sqrt{\frac{1}{n}\sum_{i=1}^n\left(w-\bar{w}\right)^2} = \sqrt{\frac{1}{n}\sum_{i=1}^n w'^2} = \sqrt{\overline{w'^2}}\ (\text{m/s}) \tag{9}$$

$$RMS\left[V'\right] = \sigma_{Total} = \sqrt{\left(RMS_u^2 + RMS_v^2 + RMS_w^2\right)}\ (\text{m/s}) \tag{10}$$

where:

$RMS\left[u'\right]$: Root-mean-square of the velocity fluctuations in streamwise direction;
$RMS\left[v'\right]$: Root-mean-square of the velocity fluctuations in lateral direction;
$RMS\left[w'\right]$: Root-mean-square of the velocity fluctuations in vertical direction and;
$RMS\left[V'\right]$: Resultant formed from the individual *RMS* values for each component.

These *RMSs* were used to determine relative turbulent intensities which are the ratios of root mean square of the velocity fluctuations to the mean velocity [30] and [31]. They indicate the fraction of the total energy of the flow which resides in the turbulent regime.These relative turbulence intensities of turbulence were analyzed as very high turbulence (>50%), high turbulence (20% - 50%), medium turbulence (5% - 20%) and low turbulence (below 5%) [32].

$$T_u = \frac{RMS\left[u'\right]}{\bar{u}} * 100;\ T_v = \frac{RMS\left[v'\right]}{\bar{v}} * 100;\ T_z = \frac{RMS\left[w'\right]}{\bar{w}} * 100;\ T_{Total} = \frac{RMS\left[V'\right]}{V_{Total}} * 100 \tag{11}$$

The Win ADV computes also the sample covariances, which were interpreted as the measure of the correlation between two variables. The sampled data covariances for all three-velocity combinations in three planes (*Cov*-XY, *Cov*-XZ, *Cov*-YZ) were the parameters used in the analysis of Reynolds shear stresses.

$$Cov(u,v) = \overline{u'v'} = \frac{1}{n}\sum_{1}^{n}(u-\bar{u})(v-\bar{v}) = \frac{1}{n}\sum_{1}^{n}u'v' \left(\mathrm{m}^2/\mathrm{s}^2\right) \quad (12)$$

$$Cov(u,w) = \overline{u'w'} = \frac{1}{n}\sum_{1}^{n}(u-\bar{u})(w-\bar{w}) = \frac{1}{n}\sum_{1}^{n}u'w' \left(\mathrm{m}^2/\mathrm{s}^2\right) \quad (13)$$

$$Cov(v,w) = \overline{v'w'} = \frac{1}{n}\sum_{1}^{n}(v-\bar{v})(w-\bar{w}) = \frac{1}{n}\sum_{1}^{n}v'w' \left(\mathrm{m}^2/\mathrm{s}^2\right) \quad (14)$$

The post-processed data from Win ADV were manipulated by Excel for better interpretation. The following parameters were computed with excel.

3.4.4. Water Flow Regime Properties

The surface roughness of flume's banks was calculated from the famous Manning's formula. In defining the flow regime before taking measurements, the flow dimensionless quantities (Reynolds' number and Froude number) were calculated. The Froude number is a good indicator of flow regime in the open channel. This number shows the status of flow like supercritical (Fr > 1), subcritical (Fr < 1) and critical (Fr = 1) while Reynolds shows the types of fluid flows in channel as categorized into three types of flow (laminar with Re < 2000, transitional with 2000 ≤ Re ≤ 4000 and turbulent with Re ≥ 4000). In quantification of impact of different vegetations on the magnitude of Manning's coefficient of roughness, the vegetation properties and water flow parameters were incorporated into the following expression [33]:

$$n = R_h^{2/3}\left[\frac{C_d * \delta}{2g}\right]^{1/2} \quad \text{with} \quad Cd = \frac{v^*}{\bar{v}} \quad \text{and} \quad v^* = \sqrt{ghS} \quad \text{and} \quad R_h = \frac{A_w}{P_w} \quad (15)$$

$$\delta = \frac{N * D}{A} \quad \text{when} \quad h \le h_s \quad \text{or} \quad \delta = \frac{N\left[2Dh_s + (h-h_s) * L_w\right]}{2Ah} \quad \text{for} \quad h > h_s \quad (16)$$

$$\mathrm{Re} = \frac{4\bar{u}R_h}{\upsilon} \quad \text{with} \quad \upsilon = \frac{\mu}{\rho}(\mathrm{m/s}) \quad \text{and} \quad (17)$$

$$\mathrm{Fr} = \frac{\bar{u}}{\sqrt{gh}} \quad (18)$$

$$v = \frac{1}{n} * R_h^{2/3} * S^{1/2} \ (\mathrm{m/s}) \quad \text{Manning's formula} \quad (19)$$

where:

When δ is vegetation density (No./m^2); D = stem diameter; h = water flow depth; h_s = vegetation height (m); A = area of the testing reach (sq.m); N = total number of stems and L_w width of wetted foliage (m), v^* is shear velocity (m/s); Cd = drag coefficient (−); $\bar{v}$ is mean velocity of the flow measured in the streamwise direction in the vegetated section; h is the water depth in the flume; S is the flume bed slope and g is the gravitational acceleration which is about 9.81 m/s^2 at the surface of the earth; R_h is hydraulic radius, which is to the ratio of wetted cross-sectional area (A_w) to wetted perimeter (P_w); n is the Manning's coefficient of roughness; υ kinematic viscosity (m^2/s); μ is dynamic viscosity of the fluid in N.s/m^2; ρ = density of the fluid in [kg/m^3], $\bar{u}$ = Mean streamwise velocity (m/s) and h is mean water depth in the channel (m).

3.4.5. Three Components of Reynolds Stresses

These were calculated as defined by the following equations [34]:

$$\tau_{uv} = -\rho * \overline{u'v'} = -\rho * Cov(u,v) \quad (\text{in N/m}^2) \quad (20)$$

$$\tau_{uw} = -\rho * \overline{u'w'} = -\rho * Cov(u,w) \quad (\text{in N/m}^2) \quad (21)$$

$$\tau_{vw} = -\rho * \overline{v'w'} - \rho * Cov(v, w) \quad (\text{in N/m}^2) \tag{22}$$

3.4.6. Turbulent Kinetic Energy (TKE)

The root mean squares of the streamwise, cross-stream, and vertical velocities (*RMSu*, *RMSv*, *RMSw*) for each time series were used to estimate *TKE* [35] and [36]. *TKE* values were evaluated to represent the average three-dimensional turbulence intensity and their cross-sectional distribution represents the antagonistic relationship between the reduced velocity and increased turbulence generated by the addition of vegetation on stream banks.

$$TKE = \frac{1}{2}\rho\left(RMS_{u'}^2 + RMS_{v'}^2 + RMS_{w'}^2\right) \quad \text{in (N/m}^2) \tag{23}$$

where:

ρ is the fluid-mixture density (assumed to equal 1000 kg/m^3).

4. Results and Discussion

4.1. Impact of Vegetations on Water Flow Velocities

In all test series, the Reynolds numbers (Re) were found to be approximately 124,732, indicating that the entire test runs are within the range of turbulent flows (124,732 > 4000) and the Froude numbers, Fr, ranged from 0.020 to 0.0604, which showed that all the test runs were carried out in subcritical flow conditions. Appendix 3 and Appendix 4 summarized water flow properties and series of all experimental treatments respectively. All measured water flow velocity values were summarized as shown in Appendix 5. The vertical distribution of velocities showed that addition of vegetations on river banks converged water flow velocities in the center of vegetated section. This behavior showed that instead of water to train on river banks, it finds its own way in the center.

This has made the banks to not lose much soil.

It also was observed that water profiles were divided into three layers or zones: upper layer above leaves when plants are submerged, mid-layer which coincides with leaves and lower layer hitting the stems. This last one is from the bed to the beginning of leaves (Figure 17). The above layers were defined depending on situation in which vegetations were with report to water flow depths (fully or partially submerged). At the top of velocity

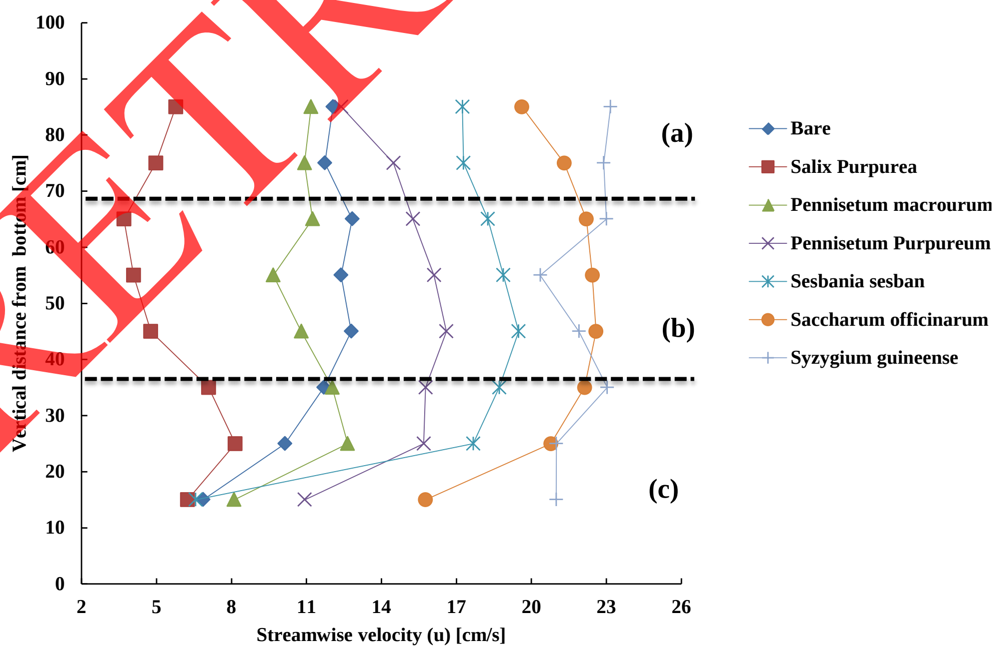

Figure 17. Velocity profiles in the vegetated mid-section reach at the centre of channel showing top layer (a), mid-layer (b) and bottom layer (c).

profile, there was a curl curved backward. This curl was caused by the wind forces acting in direction of water flow.

Figure 17 showed that the bare treatment presented the normal velocity profile progression because it was taken at the same position before insertion of vegetations.

The *Salix purpurea* and *Pennisetum macrourum* started bending when profile reached the foliage.

With help of equations (Equation (14) and Equation (15)), it was found that there was a strong relationship between total turbulence caused by insertion of vegetations in the channel and velocity profiles. The insertion of vegetations has increased the river bank roughness, which, in turn, reduced the flow velocities and as shown in Appendix 4, the manning's roughness coefficients ranges were different for all treatments and were ranging from 0.008 to 0.039 compared to assumed value of 0.020.

From Figure 18, it was noticed that for all measurements taken for bare bank treatments in all sections (upstream, middle and downstream) resulted in almost equal flow velocity values. Figure 18 and Figure 19 showed that leafy vegetation species (*Salix purpurea* and *Pennisetum macrourum*) increased surface roughness of the channel banks while others (*Saccharum officinarum* and *Syzygium guineense*) reduced it dramatically due to some of their characteristics diameters and rigidity. The vegetations with dig diameters have increased the splashing velocity as water hit their stems, which removed the soil particles to flow downstream while leafy vegetations made the flow smooth on the banks by resisting to water flow dragging forces.

4.2. Effects of Vegetations on Water Flow Turbulence Characteristics

The turbulent intensities (*RMSu'*, *RMSv'* and *RMSw'*) were calculated using equations (Equations (7)-(10)) for

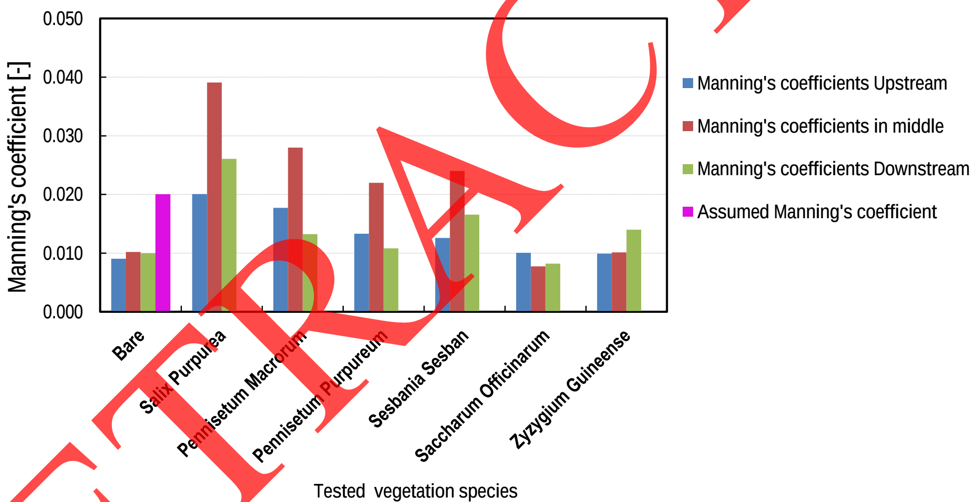

Figure 18. River bank surface roughness coefficients for the studied vegetation species.

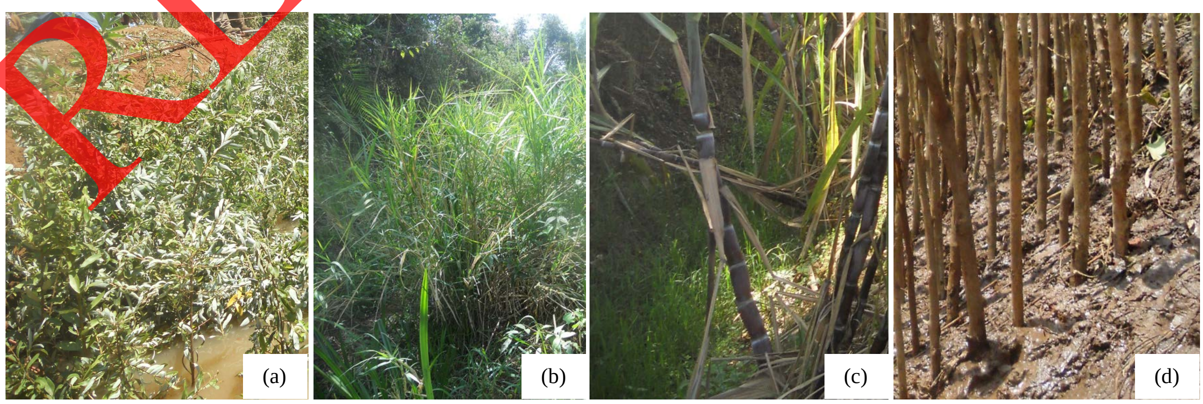

Figure 19. The vegetation properties showed high impact on flow velocities (a) and (b) and low impact for others (c) and (d) by increase or decrease of surface rougness responses.

each velocity component (u', v' and w') to show how the velocities varied from the mean. Even though the *RMS* values can be considered a measure of the violence of the turbulence fluctuations in terms of relative turbulence intensities obtained by diving them by the mean velocity (Equation (11)), interpretation of turbulence intensities remained crucial. Their calculations were summarized in **Appendix 6**.

As it can be viewed from **Figure 20**, the magnitudes of *RMSw'* (vertical turbulences) were less than the magnitudes of *RMSu'* (Streamwise turbulences) and *RMSv'* (lateral turbulences) for all vegetation types. The total turbulence intensities as calculated with Equation (10) were found to high for almost all vegetations. The streamwise turbulences were found to be slightly higher than spanwise turbulences. In short, it was found that addition of vegetations has increased turbulences.

4.3. Impact of Vegetations on Turbulent Kinetic Energy and Reynolds Shear Stresses

The turbulent kinetic energy (*TKE*) values were calculated with Equation (23) and the Reynolds stresses which are fluctuating forces, were calculated with equations (Equations (20)-(22)). These Reynolds stresses were analysed in three planes according to the three-dimensional velocity types collected with Acoustic Doppler Velocimeter: streamwise, vertical and lateral Reynolds stresses. The lateral stresses are responsible for fluvial erosion because they are generated when water flow velocities hit on river banks and start removing soil particles. The streamwise and vertical momentum exchanges between the main channel and the vegetated section can present impacts on stream bed scouring. With minutious observations, the lateral momentum transfer towards the streambank was found to be small for all profiles of mid-section, the vegetated section, compared to that of upstream and downstream sections considered as un-vegetated sections. This was an indicator that vegetations can undoubtedly protect riverbanks from eroding. Species of big diameters were judged ineffective to reduce fluctuating forces because of causing high turbulences and splashing velocities. The lateral stresses were found to be the main stressor for all tested species. This judgment was made with help of the calculations presented in **Appendix 7**.

Figure 21 showed that addition of vegetation has increased turbulent energies in the channel. The *TKE* values were lower (approximately 0.5730 N/m^2) for stream bare banks and high for *Salix purpurea* (approximately 1.2136 N/m^2).The cross-sectional distribution of *TKE* values and velocities characterizes the responsive relationship between the fluctuation and turbulences generated by the addition of streambank vegetations. *TKE* values were shifted away from the streambank by all treatments except *Salix purpurea* which showed a *TKE* value of 0.99 N/m^2 at the streambank and 0.34 N/m^2 in center of the channel. The three vegetations *Pennisetum macrourum*, *Syzygium guineense* and *Saccharum officinarum* have produced highest *TKE* values of around 1.77 N/m^2, 2.01 N/m^2 and 1.39 N/m^2 respectively (**Figure 22**). The cross-sectional distribution of velocities showed the high magnitudes in center of the channel corresponding to high *TKE* values while near stream bank, velocities and *TKE* values were very low. This was indicator that the turbulences in center found their way easily in the

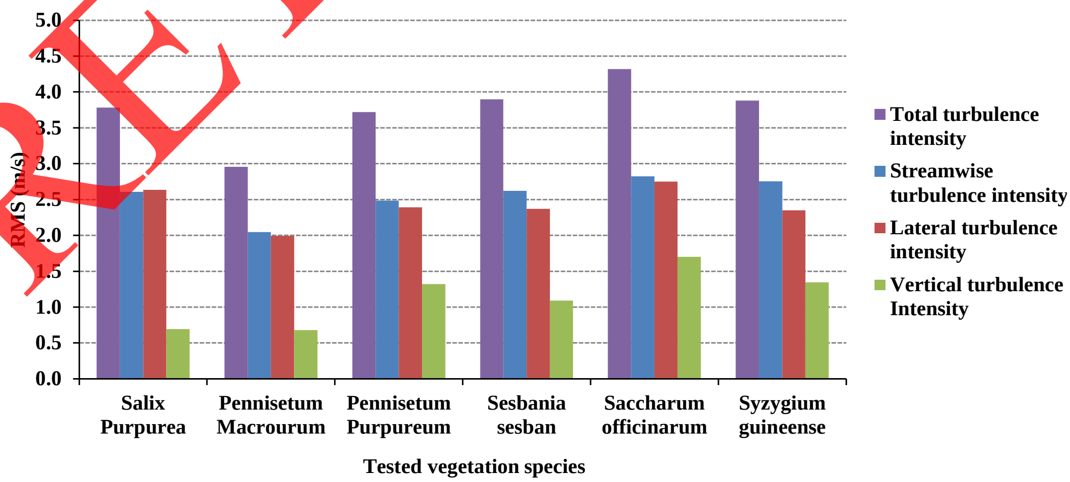

Figure 20. Comparison of three dimensional turbulence intensity magnitudes in vegetated section of sampling reach.

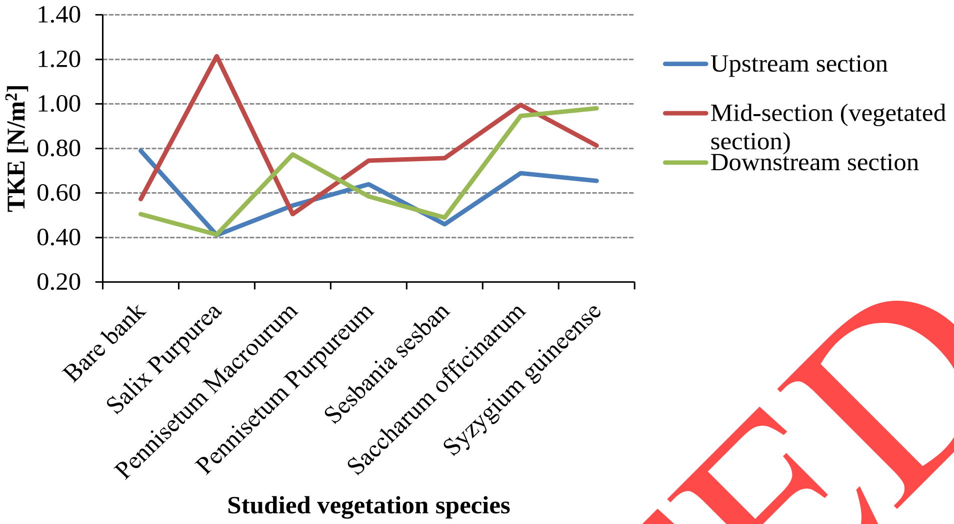

Figure 21. The comparison of TKE values for two unvegetated sections (upstream and downstream) with the vegetated mid- section.

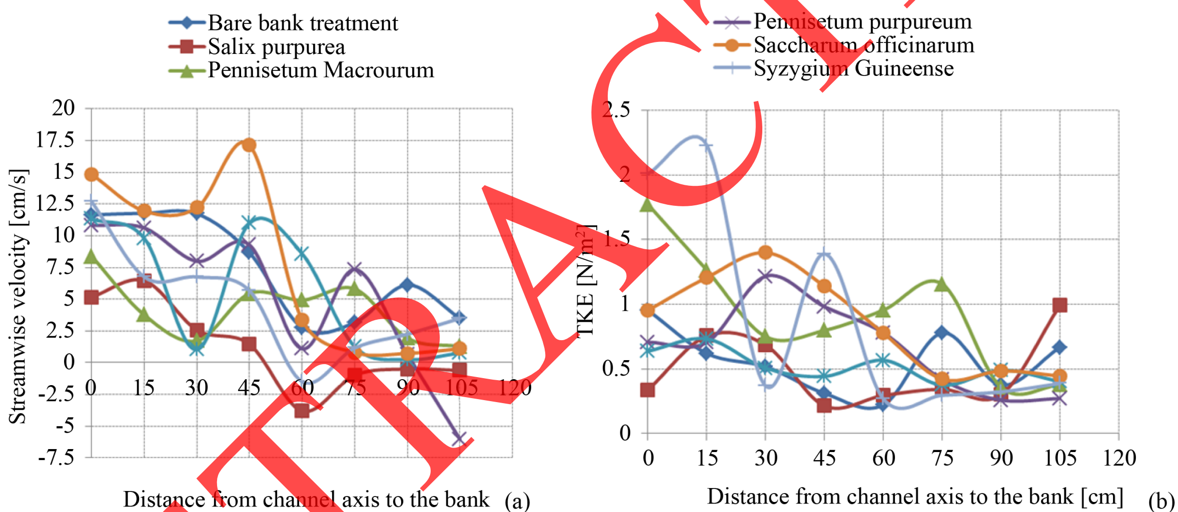

Figure 22. The comparison of cross-sectional distribution of streamwise velocities (a) TKE estimates (b) for all treatments at a water depth of 85 cm in center of vegetated section in the testing flume.

streamwise direction by keeping streambank safe from fluctuating forces.

From **Figure 23(a)**, in upstream section before water reached the vegetated section, the lateral stresses were found to be high for *bare bank* (approximately 0.0931 N/m^2) and *Saccharum officinarum* (approximately 0.0685 N/m^2), vertical momentum transfers were negatively high and streamwise stresses were found small in magnitude for all treatments. After water left the vegetated section, the lateral stresses continued to be high for bare bank and for the species with big diameters like *Saccharum officinarum* and *Syzygium guineense* (**Figure 23(b)**). Comparing upstream, middle (vegetated section) and downstream lateral stresses, it was found that the lateral stresses, responsible for removal soil particles from river banks, were minimized in vegetations with small diameters and high stem densities like in *Salix purpurea* (nearly −0.0216 N/m^2), *Pennisetum macrourum* (nearly −0.0005 N/m^2), *Sesbania sesban* (nearly 0.0010 N/m^2) and *Pennisetum Purpureum* (nearly 0.0438 N/m^2) while bare bank (about 0.0822 N/m^2), *Saccharum officinarum* (about 0.1877 N/m^2) and *Syzygium guineense* (approximately 0.1024 N/m^2) continued to induce maximum stresses on banks (**Figure 23(c)**). This was an indicator that when water hit bare bank or the stems of *Saccharum officinarum* and *Syzygium guineense*, they acquired high energies, which interacted with the removal of soil particles, the starting point of erosion. All vegetations in mid-section exhibited low magnitudes of vertical and streamwise shear stresses. Finally, a quick observation of

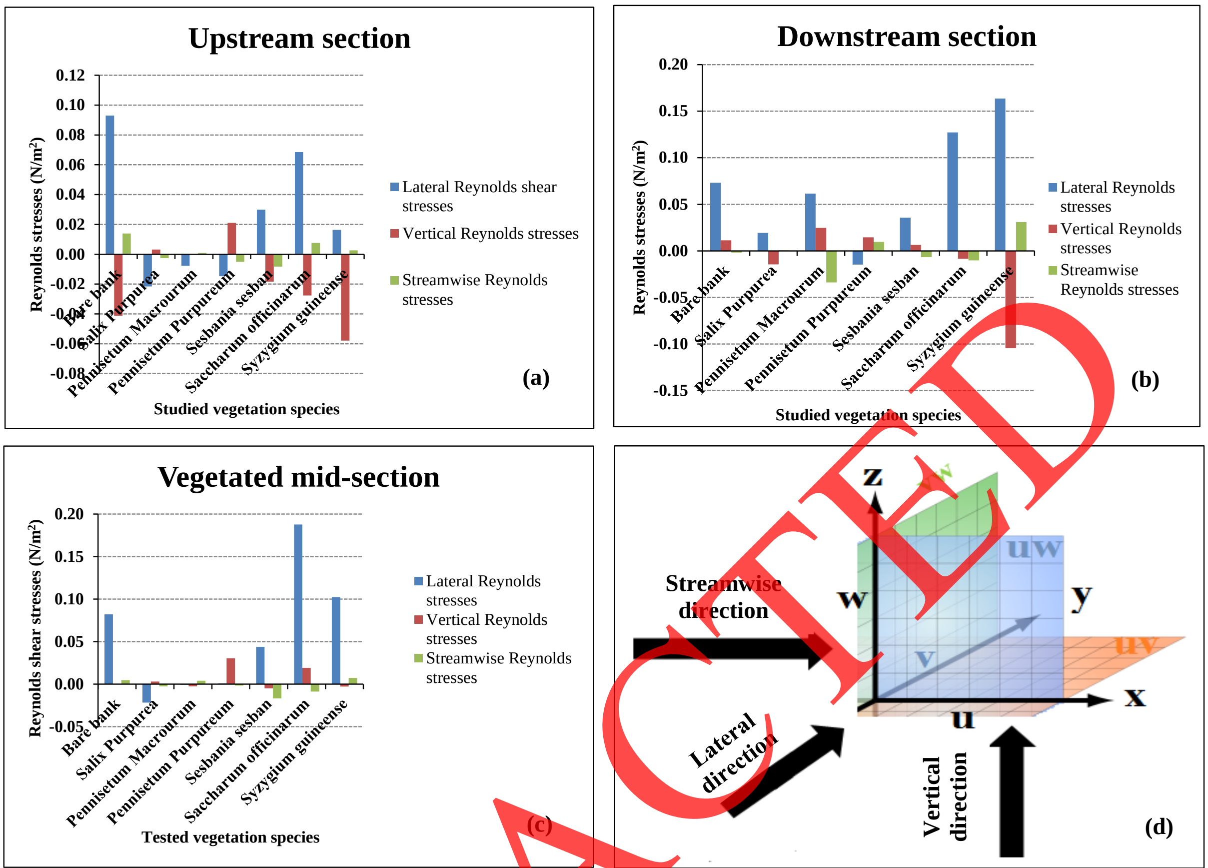

Figure 23. The comparison of Reynolds stresses (lateral, vertical and streamwise) for three sections (upstream (a), middownstream (b) and mid (c)) in three planes (d) in the flume.

performance and effectiveness of different treatments led us to the ranking of vegetations from higher to lower as follows: 1) *Salix purpurea*, 2) *Pennisetum macrourum*, 3) *Sesbania sesban*, 4) *Pennisetum purpureum*, 5) *bare bank*, 6) *Syzygium guineense* and 7) *Saccharum officinarum*.

5. Conclusions and Recommendations

On basis of the experimental analysis of seven studied streambank conditions: no vegetation (*bare bank*), bank with *Salix purpurea*, *Pennisetum purpureum*, *Pennisetum macrourum*, *Sesbania sesban*, *Saccharum officinarum* and *Syzygium guineense* and tested vegetation parameters on their effectiveness in reducing water flow velocities on channel banks under the same flow conditions (**Appendix 4**), it was that riparian vegetations could contribute much to protecting river banks from eroding provided the plant characteristics and planting arrangements were analyzed well. This contribution should be well managed to increase their effectiveness by good judgment on which species is to be grown and how to grow it. The following vegetation species (*Salix purpurea*, *Pennisetum purpureum*, *Pennisetum macrourum* and *Sesbania sesban*) were found to be more effective by reducing drastically lateral Reynolds stresses, responsible for erodibility of the river banks while *Saccharum officinarum* and *Syzygium guineense* showed opposite responses due to their big diameters and their low stem densities (**Figure 23(c)**). As it is described in Equation (15) and Equation (16), it is logical that on 1 m^2 if number of stems increases, diameter decreases and when diameters decrease, the stem densities increase with increase of surface roughness, which, in turn, contributes to reduction of velocity by considering Equation (19).

This research was intended to improve our understanding of the role of riparian vegetation in alleviating higher water flow velocities near river banks and its current findings evidenced that vegetation species added on stream banks performed differently due to their natural characteristics (type, stem diameter, stem density, leafiness, flexibility and planting arrangement). In order to consider riparian vegetations as one of the Best Management Practices (BMPs) for effective erosion and sediment generation control, it was found that there was a need to play with their characteristics. These state-of-the-art mitigation measures include establishing and maintaining effective vegetation for short-term first growth and for long-term establishment, using project scheduling and planning to reduce vegetation disturbance (particularly during the rainy season), as well as stabilizing disturbed riverbank soils to stop and prevent continued erosion and sedimentation. So, with all these above mentioned facts, we conclude by recommending Ethiopian Electric Power Corporation (EEPCO) which has hydropower dams in its attributions to work hand in hand with Ethiopian Ministry of Agriculture and Natural Resources (MoANR) which has agriculture in its attributions to mobilize the population to grow multi-purpose vegetations (economically and environment-friendly species) along the rivers that pass in their lands as agricultural activities are main contributors of sediment loading in rivers. Once this recommendation is implemented from upstream to downstream for all rivers, problems of river bank erosion and sediment loading will be progressively solved and this solution will lead to healthier dams and good environmental landscapes.

As implementation of the projects to fight against the fluvial erosion is an intensive program, these two institutions can initiate the community works by involving participatorily local people in this intensive important problem. They should start by sensitizing them about bad sides of sediments loading in rivers and encouraging them to grow vegetation species that have economical inputs to motivate them. This initiative program can allow covering a big area of river bank restoration.

The studied vegetations were selected because of their performance in stabilizing river banks and their additive economical inputs to the people:

- Sugarcane (*Saccharum officinarum*): it is a grass with key of being commercial plant for industrial production, domestic consumption, and fodder for animal.

It presents a good root system that interlocks soil particles to not degrade.

- Elephant grass (*Pennisetum purpureum*): an internationally known grass to grow along gullies and riverbanks. This grass is excellent fodder and used in construction of rural houses.

- Purple osier/willow (*Salix purpurea*): This indigenous, non-invasive shrub is ideal for erosion control on hillsides in grazed pasture and will also grow in moist valley bottoms, making it suitable for stream and riverbank erosion control. It grows best along riverbanks under natural condition. It can be planted in the presence of livestock and provide additional benefits like shade, shelter and fodder. It can produce excellent toothpicks and its wood may be used to make household utensils.

- African feather grass (*Pennisetum macrourum*): Indigenous grass that grows best along riverbanks in the catchment. This grass is very important fodder.

- Sesban (*Sesbania sesban*): It is a fast-growing, perennial legume tree, reaching up to 8 m. It is used as forage (grazed or cut-and-carried), good source of proteins for ruminants and as green manure.

It provides good quality firewood and fibre for cordage. It is outstanding in its ability to tolerate water logging and is ideally suited to seasonally waterlogged environments.

- Water pear (*Syzygium guineense*): species that grows best along riverbanks and gullies. Fruits are edible, fire wood, animal fodder. It is a medium-sized to large evergreen tree and usually grows up to 15 - 20 m high. It is preferred for stream banks and its wood. It usually occurs in lowland forests, in areas close to swamps and sometimes along riverbanks. It has creamy white flowers with a sweet fragrance that can attract bees.

Both its fruits and leaves are edible; the pulp and the fruit skin are sucked and the seed discarded. In southern Ethiopia, *Syzygium guineense* is a much-appreciated shade tree for both the homestead and the home gardens.

Finally, planting patterns may also be encouraged because the plantation of scarce vegetation may not promote the retention of sediments. The vegetations should be grown in such a way that they can grow by forming riparian buffer zones. These are zones formed with well-planted vegetations along streams, river, lakes and wetlands, and designed for stabilizing stream banks, filtering storm water runoff, providing wildlife aquatic habitats and protecting water in infiltration zones. These zones are recommended to have a width of 10 - 20 cm [37]. There should be also management of highlands by digging rainwater retaining trenches (RWRTs) and planting vegetations on top of them. Local authorities should organize seasonal and emergent tours around rivers and streams in their zones for checking whether water in river is not flowing well and undertake some urgent activities to clear away obstacles obstructing water ways.

Acknowledgements

The work described and reported here was undertaken as part of Mr. Ayalew Talema Legass's research work within the IUC-JU cooperation research programme with Jimma University "soil fertility conservation and sediment control project" that was focusing on the impact of the Gilgel Gibe hydro-electric dam in terms of human and animal health, ecology and agronomy. It was carried out under the umbrella of the Flemish Interuniversity Council (VLIR-UOS), Belgium. Project leaders: North (Belgium) represented by Prof. Jan Diels, KU Leuven and South (Ethiopia) represented Mr. Amsalunebiyu, Jimma University.

The authors wish to acknowledge the support of Jimma University, through its college of Agriculture and veterinary medicine (JU-CAVM) for having facilitated the to- and fro-transport to the study area and assisted tirelessly in the supply of equipment and materials. The authors also express their gratitude to the local authority of Seka Chekorsa district (Oromia regional state) for having allowed us to have access to the study area and work from there under secured conditions.

References

[1] Gebresenbet, T.S. (2015) Modeling of Cascade Dams and Reservoirs Operation for Optimal Water Use: Application to Omo Gibe River Basin, Ethiopia.

[2] Devi, R., Tesfahune, E., Legesse, W., Deboch, B. and Beyene, A. (2008) Assessment of Siltation and Nutrient Enrichment of Gilgel Gibe Dam, Southwest Ethiopia. *Bioresource Technology*, **99**, 975-979. http://dx.doi.org/10.1016/j.biortech.2007.03.013

[3] Hooke, J.M. (1979) An Analysis of the Processes of River Bank Erosion. *Journal of Hydrology*, **42**, 39-62. http://dx.doi.org/10.1016/0022-1694(79)90005-2

[4] Li, Y., Wang, Y., Anim, D.O., Tang, C., Du, W., Ni, L., Acharya, K., *et al.* (2014) Flow Characteristics in Different Densities of Submerged Flexible Vegetation from an Open-Channel Flume Study of Artificial Plants. *Geomorphology*, **204**, 314-324. http://dx.doi.org/10.1016/j.geomorph.2013.08.015

[5] Abernethy, B. and Rutherford, I.D. (2000) The Effect of Riparian Tree Roots on the Mass-Stability of Riverbanks. *Earth Surface Processes and Landforms*, **25**, 921-937. http://dx.doi.org/10.1002/1096-9837(200008)25:9<921::AID-ESP93>3.0.CO;2-7

[6] Abernethy, B. and Rutherfurd, I.D. (2001) The Distribution and Strength of Riparian Tree Roots in Relation to Riverbank Reinforcement. *Hydrological Processes*, **15**, 63-79. http://dx.doi.org/10.1002/hyp.152

[7] Laflen, J.M., Foster, G.R. and Onstad, C.A. (1985) Simulation of Individual-Storm Soil Loss for Modeling the Impact of Soil Erosion on Crop Productivity. In: El-Swaify, W.C.S.A., Ed., *Soil Erosion and Conservation*, Soil Conservation Society of America, Ankeny, 285-295.

[8] Vought, L.B.M., Pinay, G., Fuglsang, A. and Ruffinoni, C. (1995) Structure and Function of Buffer Strips from a Water Quality Perspective in Agricultural Landscapes. *Landscape and Urban Planning*, **31**, 323-331. http://dx.doi.org/10.1016/0169-2046(94)01057-F

[9] Carollo, F.G., Ferro, V. and Termini, D. (2002) Flow Velocity Measurements in Vegetated Channels. *Journal of Hydraulic Engineering*, **128**, 664-673. http://dx.doi.org/10.1061/(ASCE)0733-9429(2002)128:7(664)

[10] Parkyn, S.M., Davies-Colley, R.J., Halliday, N.J., Costley, K.J. and Croker, G.F. (2003) Planted Riparian Buffer Zones in New Zealand: Do They Live up to Expectations? *Restoration Ecology*, **11**, 436-447. http://dx.doi.org/10.1046/j.1526-100X.2003.rec0260.x

[11] Winward, A.H. (2000) Monitoring the Vegetation Resources in Riparian Areas. Gen. Tech. Rep., RMRSGTR-GTR-47.

[12] Auel, C., Albayrak, I. and Boes, R.M. (2013) Turbulence Characteristics in Supercritical Open-Channel Flows: Effects of Froude Number and Aspect Ratio. *Journal of Hydraulic Engineering*, **140**, Article ID: 04014004.

[13] Ian, R., Anderson, B. and Ladson, A. (2007) Managing the Effects of Riparian Vegetation on Flooding. In: Lovett, S. and Price, P., Eds., *Principles for Riparian Lands Management*, Land and Water Australia, Canberra, 63-84.

[14] Järvelä, J. (2005) Effect of Submerged Flexible Vegetation on Flow Structure and Resistance. *Journal of Hydrology*, **307**, 233-241. http://dx.doi.org/10.1016/j.jhydrol.2004.10.013

[15] Connecticut River Joint Commissions (CRJC) (1998) Introduction to Riparian Buffers. Connecticut River Joint Commissions. http://www.crjc.org/buffers/Introduction.pdf

[16] Hooke, J. (1980) Magnitude and Distribution of Rates of River Bank Erosion. *Earth Surface Processes and Landforms*, **5**, 143-157. http://dx.doi.org/10.1002/esp.3760050205

[17] Macfall, J., Robinette, P. and Welch, D. (2014) Factors Influencing Bank Geomorphology and Erosion of the Haw River, a High Order River in North Carolina, Since European Settlement. *PloS ONE*, **9**, e110170. http://dx.doi.org/10.1371/journal.pone.0110170

[18] Stream Processes (2014) http://www.columbia.edu/~vjd1/streams_basic.htm

[19] Broothaerts, N., Kissi, E., Poesen, J., van Rompaey, A., Getahun, K., Van Ranst, E. and Diels, J. (2012) Spatial Pat-

terns, Causes and Consequences of Landslides in the Gilgel Gibe Catchment, SW Ethiopia. *Catena*, **97**, 127-136. http://dx.doi.org/10.1016/j.catena.2012.05.011

[20] Wilcox, A.C. and Wohl, E.E. (2007) Field Measurements of Three-Dimensional Hydraulics in a Step-Pool Channel. *Geomorphology*, **83**, 215-231. http://dx.doi.org/10.1016/j.geomorph.2006.02.017

[21] Mertens, K. (2013) Land Use Dynamics in the Planosol Belt of the Gilgel Gibe Catchment, South-West Ethiopia. http://lib.ugent.be/fulltxt/RUG01/002/063/605/RUG01-002063605_2013_0001_AC.pdf

[22] EEPLA (1996) Ethiopia—The Gilgel Gibe Hydroelectric Project Resettlement Plan. 176 p.

[23] SonTek and YSI (2001) SonTek/YSI ADVField/Hydra Acoustic Doppler Velocimeter (Field) Technical Documentation. ADV Field User Manual, S Water flow, Quality and Quantity Sampling and Monitoring Meters and Instruments. onTek/YSI Inc., San Diego.

[24] SonTek (2001) SonTek/YSI ADVField/Hydra Acoustic Doppler Velocimeter (Field) Technical Documentation. San Diego, California, USA.

[25] Velasco, D.W. and Huhta, C.A. (2009) Experimental Verification of Acoustic Doppler Velocimeter (ADV®) Performance in Fine-Grained, High Sediment Concentration Fluids. San Diego, California, USA.

[26] SonTek (2008) SonTek 10MHz-ADV Expanded Description. http://www.elscolab.com/sites/elscolab/files/uploads/37/SonTek_ADV_AcousticDopplerVelocimeter_ExpandedDescription.pdf

[27] Hickin, E.J. (2004) The Nature of Turbulence and Velocity Distributions in Rivers. In: Hickin, E.J., Ed., *River Hydraulics and Channel Form*, Chapter 5, Wiley, Chichester, 5.1-5.19. http://www.sfu.ca/~hickin/FLUIDS/Chapt5-Turbulence.pdf

[28] Pugh, C.A. (2015) Win ADV Manual.

[29] Nikora, V. and Goring, D. (2002) Fluctuations of Suspended Sediment Concentration and Turbulent Sediment Fluxes in an Open-Channel Flow. *Journal of Hydraulic Engineering*, *ASCE*, **128**, 214-224. http://dx.doi.org/10.1061/(ASCE)0733-9429(2002)128:2(214)

[30] Hopkinson, L. and Wynn, T. (2009) Vegetation Impacts on Near Bank Flow. *Ecohydrology*, **2**, 404-418. http://dx.doi.org/10.1002/eco.87

[31] Manshadi, M.D. (2011) The Importance of Turbulence in Assessment of Wind Tunnel Flow Quality. In: Lerner, V.J.C. and Boldes, U., Eds., *Wind Tunnels and Experimental Fluid Dynamics Research*, Chapter 12, InTech, 261-278. http://www.intechopen.com/books/wind-tunnels-and-experimental-fluid-dynamics-research/the-importance-of-turbulence-reduction-in-assessment-of-wind-tunnel-flow-quality http://dx.doi.org/10.5772/17069

[32] Johnson, R.W. (1998) The Handbook of Fluid Dynamics. Vol. I, CRC Press Llc., Boca Raton, 21-21.

[33] Xia, J. and Nehal, L. (2013) Hydraulic Features of Flow through Emergent Bending Aquatic Vegetation in the Riparian Zone. *Water*, **5**, 2080-2093. http://dx.doi.org/10.3390/w5042080

[34] Schlichting, H. and Gersten, K. (2000) Boundary-Layer Theory. 8th Edition, Springer-Verlag, Berlin.

[35] Clifford and French (1993) Monitoring and Modelling Turbulent Flow: Historical and Contemporary Perspectives. In: Clifford, N.J., French, J.R. and Hardisty, J., Eds., *Turbulence*: *Perspectives on Flow and Sediment Transport*, Wiley, Chichester, 1-34.

[36] Middleton and Wilcock (1994) Mechanics in the Earth and Environmental Sciences. Cambridge University Press, Cambridge.

[37] Parkyn, S. (2004) Review of Riparian Buffer Zone Effectiveness. No. 2004-2005, Ministry of Agriculture and Forestry, Wellington, New Zealand.

[38] Chen, D. and Chen, W.H. (2013) Using the Köppen Classification to Quantify Climate Variation and Change: An Example for 1901-2010. *Environmental Development*, **6**, 69-79. http://dx.doi.org/10.1016/j.envdev.2013.03.007

Appendices

Appendix 1: Site Shelter during Data Collection

Appendix 2: Screenshot Showing Horizon ADV Real-Time Data Collection Screen

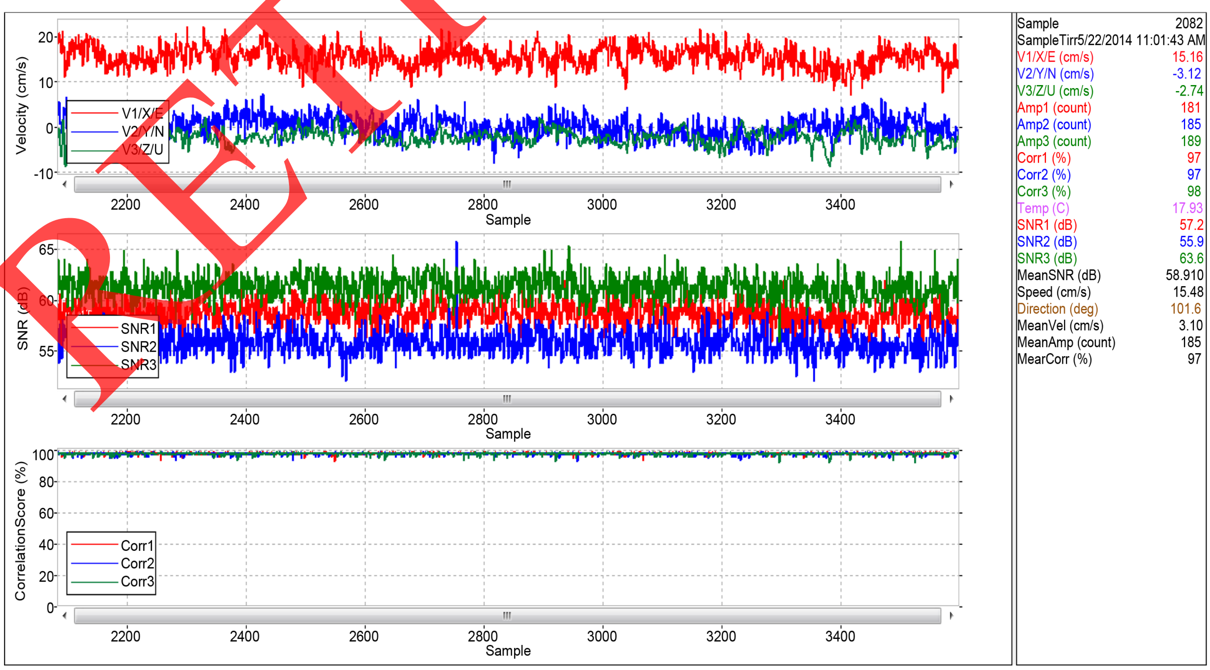

Appendix 3: Flow Properties for Experimental Treatments

	Parameters	Velocity			Discharges			Reynolds number			Froude numbers			Manning's coefficients		
	cross-ections	UPS[a]	MID[b]	DWS[c]	UPS	MID	DWS	UPS	MID	DWS	UPS	MID	DWS	UPS	MID	DWS
SN°	Species	Measured velocity [cm/s]			Q [m^3/s]			Re			Fr			n		
1	Bare	10.228	8.822	7.708	0.189	0.163	0.143	193,297	166,727	145,669	0.042	0.036	0.032	0.009	0.010	0.010
2	*Salix purpurea*	4.601	2.364	3.544	0.085	0.044	0.066	86,962	44,686	66,971	0.019	0.010	0.015	0.020	0.039	0.026
3	*Pennisetum macrorum*	5.212	4.585	6.971	0.096	0.085	0.129	98,504	86,651	131,746	0.021	0.019	0.029	0.018	0.028	0.013
4	*Pennisetum purpureum*	6.943	10.079	8.528	0.128	0.186	0.158	131,218	190,475	161,176	0.029	0.042	0.035	0.013	0.022	0.011
5	*Sesbania sesban*	7.342	9.498	5.583	0.136	0.176	0.103	138,764	179,493	105,509	0.030	0.039	0.023	0.013	0.024	0.017
6	*Saccharum officinarum*	9.197	11.912	11.227	0.170	0.220	0.208	173,816	225,125	212,181	0.038	0.049	0.046	0.010	0.008	0.008
7	*Zyzygium guineense*	9.330	9.121	6.605	0.173	0.169	0.122	176,330	172,376	124,833	0.038	0.038	0.027	0.010	0.010	0.014
	Averages				0.140	0.149	0.133	142,699	152,219	135,441	0.031	0.033	0.030	0.013	0.020	0.014
							0.140			143,453			0.031			0.016

a, Upstream of vegetated section. b, Middle of vegetated section. c, Downstream of vegetated section.

Appendix 4: Summary of Experiments Performed for Vegetation Density Series

SN°	Test runs	Description	Cross-sections	Profiles	Data pts	Q (m^3/s)	ui (m/s)	h (cm)	Re	Fr
						Properties of incoming flow in SS				
1			Up, SS	3 Ps, 6 SLs	45	0.122	0.066	100	124,732	0.021
2	TV0 BB	No Vegetation	Mid, SS	3 Ps, 6 SLs	45	0.122	0.066	100	124,732	0.021
3			Down, SS	3 Ps, 6 SLs	45	0.122	0.066	100	124,732	0.021
4			Up, SS	3 Ps, 6 SLs	45	0.122	0.066	100	124,732	0.021
5	TV1 PP	49 Plant stems/m^2	Mid, SS	3 Ps, 6 SLs	45	0.122	0.066	100	124,732	0.021
6			Down, SS	3 Ps, 6 SLs	45	0.122	0.066	100	124,732	0.021
7			Up, SS	3 Ps, 6 SLs	45	0.122	0.066	100	124,732	0.021
8	TV2 PM	256 Plant stems/m^2	Mid, SS	3 Ps, 6 SLs	45	0.122	0.066	100	124,732	0.021
9			Down, SS	3 Ps, 6 SLs	45	0.122	0.066	100	124,732	0.021
10			Up, SS	3 Ps, 6 SLs	45	0.122	0.066	100	124,732	0.021
11	TV3 SO	25 Plant stems /m^2	Mid, SS	3 Ps, 6 SLs	45	0.122	0.066	100	124,732	0.021
12			Down, SS	3 Ps, 6 SLs	45	0.122	0.066	100	124,732	0.021
13			Up, SS	3 Ps, 6 SLs	45	0.122	0.066	100	124,732	0.021
14	TV4 SP	49 Plant stems /m^2	Mid, SS	3 Ps, 6 SLs	45	0.122	0.066	100	124,732	0.021
15			Down, SS	3 Ps, 6 SLs	45	0.122	0.066	100	124,732	0.021
16			Up, SS	3 Ps, 6 SLs	45	0.122	0.066	100	124,732	0.021
17	TV5 SS	42 Plant stems/m^2	Mid, SS	3 Ps, 6 SLs	45	0.122	0.066	100	124,732	0.021
18			Down, SS	3 Ps, 6 SLs	45	0.122	0.066	100	124,732	0.021
19			Up, SS	3 Ps, 6 SLs	45	0.122	0.066	100	124,732	0.021
20	TV6 SG	35 Plant stems/m^2	Mid, SS	3 Ps, 6 SLs	45	0.122	0.066	100	124,732	0.021
21			Down, SS	3 Ps, 6 SLs	45	0.122	0.066	100	124,732	0.021
Total	**7**	**439**	**21**	-	**945**	-	-	-	-	-

Seven treatments: TV0 BB (Treatment with no vegetation or bare soil bank), TV1 PP (Treatment with *Pennisetum purpureum*), TV2 PM (Treatment with *Pennisetum macrorum*), TV3 SO (Treatment with *Saccharum officinarum*), TV4 SP (Treatment with *Salix purpurea*), TV5 SS (Treatment with *Sesbania sesban*) and finally TV6 SG (Treatment with *Syzygium guineense*). The UPS; MID and DWS in table stand for Upstream, mid and downstream positions of sampling section (SS) with regard to vegetated section (VS).

Appendix 5: Summary of Average Velocity Values of All Points per Sampling Section

Sampling reach		**Vegetated section**											
SN°	Sections	Upstream				In middle				Downstream			
	Plant species / *Parameters*	Avg Vx	Avg Vy	Avg Vz	Mag V-Avg	Avg Vx	Avg Vy	Avg Vz	Mag V-Avg	Avg Vx	Avg Vy	Avg Vz	Mag V-Avg
		cm/s				cm/s				cm/s			
1	*Bare bank*	10.228	−2.179	1.498	10.611	8.822	−1.831	1.234	9.131	7.708	−2.110	0.809	8.181
2	*Salix purpurea*	4.601	−0.020	0.536	4.776	2.364	−2.607	0.767	3.721	3.544	−1.048	0.658	4.917
3	*Pennisetum macrourum*	5.212	0.451	−0.127	5.477	4.585	−1.188	0.721	6.411	6.971	1.046	−1.408	7.306
4	*Pennisetum purpureum*	6.943	2.412	−1.480	7.687	9.992	3.180	−1.470	10.801	8.528	1.924	0.613	8.914
5	*Sesbania sesban*	7.342	1.122	0.800	7.516	9.498	0.051	0.809	9.617	5.583	−0.388	−0.026	5.738
6	*Saccharum officinarum*	9.197	−3.127	0.914	9.819	11.912	−3.783	1.486	12.798	11.227	−1.280	1.006	11.739
7	*Syzygium guineense*	9.330	1.007	2.111	9.687	9.121	−0.082	1.051	9.392	6.605	−0.125	1.535	6.362
	Overall averages of parameters' values per sampling reach												
						Δ*Vx* (%)	Δ*Vx* (%)			Average values in three sections			
1	*Bare bank*					−13.746	−12.631			8.919	−2.040	1.180	9.307
2	*Salix purpurea*					−48.615	49.871			3.503	−1.225	0.654	4.471
3	*Pennisetum macrourum*					−12.033	52.041			5.589	0.103	−0.271	6.398
4	*Pennisetum purpureum*					43.914	−14.650			8.488	2.505	−0.779	9.134
5	*Sesbania sesban*					29.351	−41.218			7.474	0.262	0.528	7.624
6	*Saccharum officinarum*					29.520	−5.750			10.779	−2.730	1.136	11.452
7	*Syzygium guineense*					−2.242	−27.581			8.352	0.267	1.566	8.480
						U/s & mid	Mid & d/s						

Appendix 6: Summary of Turbulence Intensity Values of All Points per Sampling Section

Sampling reach		Vegetated section											
SN°	Sections	Upstream				In the middle				Downstream			
	Parameters / *Plant species*	*RMS*[*Vx*′]	*RMS*[*Vy*′]	*RMS*[*Vz*′]	*RMS*[*V*′]	*RMS*[*Vx*′]	*RMS*[*Vy*′]	*RMS*[*Vz*′]	|*RMS*[*V*′]	*RMS*[*Vx*′]	*RMS*[*Vy*′]	*RMS*[*Vz*′]	*RMS*[*V*′]
		cm/s				cm/s				cm/s			
1	*Bare bank*	2.630	2.501	1.401	3.904	2.298	2.173	1.082	3.348	2.204	2.052	0.860	3.140
2	*Salix Purpurea*	1.850	1.877	0.726	2.748	2.609	2.635	0.692	3.783	2.016	1.763	0.708	2.788
3	*Pennisetum Macrourum*	2.179	2.139	0.827	3.180	2.046	1.994	0.680	2.954	2.626	2.324	1.458	3.828
4	*Pennisetum Purpureum*	2.334	2.282	0.868	3.389	2.485	2.390	1.320	3.719	2.330	2.090	1.001	3.320
5	*Sesbania sesban*	2.060	1.983	0.940	3.024	2.621	2.371	1.092	3.896	2.179	1.968	0.895	3.092
6	*Saccharum officinarum*	2.451	2.435	1.263	3.690	2.824	2.750	1.699	4.318	2.947	2.562	1.621	4.263
7	***Syzygium guineense***	2.424	2.274	1.286	3.580	2.753	2.349	1.345	3.880	2.741	2.349	1.630	4.013

Continued

	Overall averages of parameters' values per sampling reach						
		Δ*Vx* (%)	Δ*Vx* (%)	Average values in three sections			
1	*Bare bank*	−12.654145	−4.09509836	2.377	2.242	1.114	3.464
2	*Salix Purpurea*	41.02136554	−22.714785	2.158	2.092	0.708	3.106
3	*Pennisetum Macrourum*	−6.1139629	28.37677384	2.284	2.152	0.988	3.321
4	*Pennisetum Purpureum*	6.493089712	−6.23481492	2.383	2.254	1.063	3.476
5	*Sesbania sesban*	27.21584175	−16.889092	2.287	2.107	0.976	3.337
6	*Saccharum officinarum*	15.20427495	4.358725595	2.741	2.582	1.528	4.090
7	***Syzygium guineense***	13.56035052	−0.44749447	2.639	2.324	1.420	3.824
		U/s & mid	Mid & d/s				

Appendix 7: Summary of Reynolds Shear Stress and *TKE* Values of All Points per Sampling Section

Sampling reach		**Vegetated section**											
SN°	Plant species	Upstream				In the middle				Downstream			
	Parameters / *Plant species*	*TKE*	τ_{uw}	τ_{uv}	τ_{vw}	*TKE*	τ_{uw}	τ_{uv}	τ_{vw}	*TKE*	τ_{uw}	τ_{uv}	τ_{vw}
		[N/m²]				[N/m²]				[N/m²]			
1	*Bare bank*	0.7896	0.0931	−0.0412	0.0139	0.5730	0.0822	0.0003	0.0047	0.5046	0.0731	0.0114	−0.0018
2	*Salix Purpurea*	0.4112	−0.0216	0.0032	−0.0026	1.2136	−0.0216	0.0032	−0.0026	0.4129	0.0193	−0.0144	0.0006
3	*Pennisetum Macrourum*	0.5438	−0.0078	0.0001	0.0008	0.5047	−0.0005	−0.0026	0.0040	0.7730	0.0616	0.0247	−0.0339
4	*Pennisetum Purpureum*	0.6390	−0.0148	0.0210	−0.0051	0.7459	0.0010	0.0306	−0.0014	0.5843	−0.0147	0.0147	0.0095
5	*Sesbania sesban*	0.4598	0.0300	−0.0184	−0.0083	0.7567	0.0438	−0.0048	−0.0168	0.4899	0.0357	0.0063	−0.0067
6	*Saccharum officinarum*	0.6893	0.0685	−0.0277	0.0076	0.9962	0.1877	0.0192	−0.0085	0.9463	0.1272	−0.0084	−0.0103
7	*Syzygium guineense*	0.6543	0.0164	−0.0579	0.0027	0.8132	0.1024	−0.0027	0.0073	0.9803	0.1635	−0.1045	0.0310
	Overall averages of parameters' values per sampling reach												
						Δ*TKE* (%)	Δ*TKE* (%)			Average values in three sections			
1	*Bare bank*					−27.4316762	−11.9342147			0.6224	0.0828	−0.0098	0.0056
2	*Salix Purpurea*					195.0905776	−65.9796886			0.6792	−0.0080	−0.0027	−0.0015
3	*Pennisetum Macrourum*					−7.19746425	53.17124638			0.6072	0.0178	0.0074	−0.0097
4	*Pennisetum Purpureum*					16.72715567	−21.6625174			0.6564	−0.0095	0.0221	0.0010
5	*Sesbania sesban*					64.55431555	−35.2563909			0.5688	0.0365	−0.0056	−0.0106
6	*Saccharum officinarum*					44.52343224	−5.00495552			0.8773	0.1278	−0.0056	−0.0037
7	*Syzygium guineense*					24.28102648	20.54770459			0.8160	0.0941	−0.0550	0.0137
						U/s & mid	Mid & d/s						

τ_{uw} Lateral Reynolds stresses in the plane UW bounded by coordinates X and Z (N/m^2). τ_{uv} Vertical Reynolds stresses in the plane UV bounded by coordinates X and Y (N/m^2). τ_{vw} streamwise Reynolds stresses in the plane VW bounded by coordinates Yand Z (N/m^2). Δ*TKE* Compared differences of *TKE* values from upstream and mid sections (u/s); Mid and downstream sections (d/s) For detailed descriptions of planes, see the **Figure 23**.

Appendix 8: World Map of Köppen-Geiger Climate Classification (Source: [38])

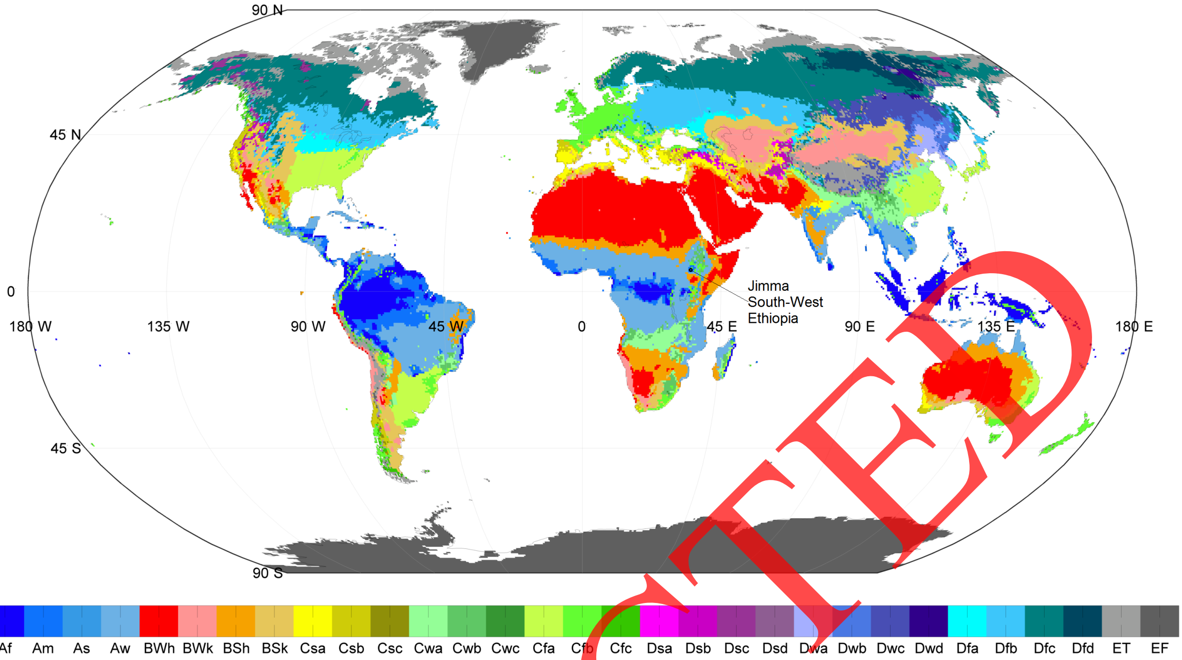

First letter	Second letter		Third letter
A: Tropical	f: Fully humid	T: Tundra	h: Hot arid
B: Dry	m: Monsoon	F: Frost	k: Cold arid
C: Mild temperate	s: Dry summer		a: Hot summer
D: Snow	w: Dry winter		b: Warm summer
E: Polar	W: Desert		c: Cool summer
	S: Steppe		d: Cold summer

Major Group	Sub-types
A: Tropical	Tropical rainforest: Af
	Tropical monsoon: Am
	Tropical wet and dry savanna: Aw
B: Dry	Desert (arid): BWh, BWk
	Steppe (semi-arid): BSh, BSk
C: Mild temperate	Mediterranean: Csa, Csb, Csc
	Humid subtropical: Cfa, Cwa
	Oceanic: Cfb, Cfc, Cwb, Cwc
D: Snow	Humid: Dfa, Dwa, Dfb, Dwb, Dsa, Dsb
	Subarctic: Dfc, Dwc, Dfd, Dwd, Dsc, Dsd
E: Polar	Tundra: ET
	Ice cap: EF